



Cite this: *Chem. Sci.*, 2024, **15**, 9874

All publication charges for this article have been paid for by the Royal Society of Chemistry

Received 20th April 2024  
Accepted 20th May 2024

DOI: 10.1039/d4sc02628d  
[rsc.li/chemical-science](http://rsc.li/chemical-science)

## 1. Introduction

Porous solids, which include zeolites, metal-organic frameworks (MOFs), covalent-organic frameworks (COFs), *etc.*, have

<sup>a</sup>*Key Laboratory of the Ministry of Education for Advanced Catalysis Materials, College of Chemistry and Materials Sciences, Zhejiang Normal University, Jinhua, 321004, P. R. China. E-mail: [jiantang.li@zjnu.edu.cn](mailto:jiantang.li@zjnu.edu.cn)*

<sup>b</sup>*Fujian Key Laboratory of Polymer Materials, College of Chemistry and Materials Sciences, Fujian Normal University, Fujian, 350007, P. R. China. E-mail: [banglin.chen@fjnu.edu.cn](mailto:banglin.chen@fjnu.edu.cn)*



Jiantang Li

*crystallized materials for gas adsorption and separation.*

*Jiantang Li received his PhD in 2019 from Jilin University under the supervision of Prof. Yunling Liu. During 2019–2023, he joined the group of Prof. Mohamed Eddaoudi as a Postdoctoral Fellow at the King Abdullah University of Science and Technology (KAUST). He is now working at Zhejiang Normal University as a Double Dragon Scholar Professor. His research focuses on the design and synthesis of novel porous*

*entered a whole new era along with the rapid development of reticular chemistry. The research of porous materials constructed *via* strong bonds (coordination bonds and covalent bonds) has advanced our understanding of functional-directed design, and the development of various synthetic tools has enriched the library of reticular chemistry. These materials possess tunable porosity and adjustable pore structures, enabling high customization and functionality, thus emerging as one of the most rapidly growing fields in chemistry and materials science.<sup>1–9</sup>*



Banglin Chen

*Banglin Chen received his BS (1985) and MS (1988) degrees in Chemistry from Zhejiang University in China, and his PhD (2000) from the National University of Singapore. He worked at the University of Michigan, Cornell University, and Louisiana State University during 2000–2003, the University of Texas at Rio Grande Valley during 2003–2009, and the University of Texas at San Antonio during 2009–2023. Now he is a university distinguished chair professor at Fujian Normal University and Zhejiang Normal University, working on multifunctional MOF, COF, and HOF materials.*



Hydrogen-bonded organic frameworks (HOFs), a novel class of porous materials, are formed by the self-assembly of organic building units *via* intermolecular H-bonding interactions. Unlike MOFs and COFs, which are constructed through strong coordination or covalent bonds, the weaker bond strength and flexible feature of H-bonds lead to challenges in terms of the stability and structural design of HOFs, but at the same time, bring about new opportunities for structural diversity and flexibility.<sup>10–22</sup> In recent years, HOFs have shown great potential in gas storage/separation, sensing, proton conduction, *etc.*

H-bonds are a type of weak supramolecular interaction characterized by an attractive force between permanent dipoles, occurring between a hydrogen atom bonded to another atom *via* a covalent bond and another electronegative atom (X–H $\cdots$ Y). Typically, the atoms (X and Y) on both sides of the hydrogen atom involved in H-bonding are highly electronegative (*e.g.*, N and O). It's worth noting that H-bonds can form both intermolecularly and intramolecularly. Although many arguments exist about H-bonds, their widespread presence and significance in chemistry, materials science, and biology have been recognized. As shown in Fig. 1, some common H-bond motifs used for constructing HOFs include carboxyl dimer, guanidinium-sulfonate, pyrazole, benzimidazolone, amidinium-carboxylate, 2,4-diaminotriazine, 2,6-diaminopurine, *etc.* For these typical H-bonds, the bond lengths (X–H $\cdots$ Y, distance between X and Y) usually range from 2.5 to 3.2 Å, much longer than the 1.2–1.5 Å typically found in covalent bonds. Therefore, the flexibility of H-bonding is one of its essential features in terms of strength and angle.

Open frameworks based on H-bonds have been reported as early as 1914,<sup>23</sup> and along with the development of single-crystal diffraction techniques, many related structures have been published since then. However, most of them have remained at the level of structural characterization; this may be due to the lack of in-depth understanding and effective activation methods in the early days, similar to the challenges faced in the early development of MOFs.<sup>24</sup> In 2011, Chen *et al.* successfully achieved the activation of HOF-1, a compound that was reported more than a decade ago *via* a 2,4-diaminotriazine moiety,<sup>25,26</sup> using a solvent exchange strategy, demonstrating for

the first time the permanent porosity and flexibility of this type of material. They also discovered its potential application in gas separation as the first representative of a functional HOF.<sup>27</sup> In the same period, Schröder *et al.* reported another example of a supramolecular organic framework (SOF-1) with permanent porosity, marking the official beginning of the era of rapid development of HOFs.<sup>28</sup>

Flexibility is one of the most fascinating features of porous materials, especially evident in flexible MOFs and COFs.<sup>29–34</sup> Much of the flexibility of HOFs comes from the weak H-bonding strength and the wide range of H-bond angles (from 130° to 180°). In some cases, this angle even approaches 90°.<sup>11</sup> Such a flexibility of H-bonding will significantly affect the structural diversity of HOFs. Functional modification of organic motifs is a very effective method to regulate the H-bonding patterns by using steric hindrance or planarity changes. As in the case of HOF-BTB, HOF-22 and PFC-12, the organic units are similar, but the effects of functionalization result in completely different structures.<sup>35–37</sup> Even for the same organic motifs, changing solvents/conditions could have a considerable impact on H-bonding patterns during crystallization (Fig. 2). For example, the rapid recrystallization of tris(4-carboxyphenyl)amine (TCA) in methanol can result in HOF-16 with free –COOH sites in the channel, whereas it can lead to HOF-11 in THF/hexane with an inert pore surface.<sup>38</sup> The flexibility in the self-assembly process has greatly increased the diversity of HOFs while posing challenges for targeted synthesis. In 2011, Cooper *et al.* demonstrated that the complicated assembly of porous cages can be precisely predicted by lattice energy calculations, which exhibited the application of “design by computational selection” for porous organic frameworks.<sup>39</sup> Therefore, scientists have always remained hopeful of controlling the flexible and complex self-assembly behavior and mastering effective strategies for targeting and constructing HOFs. Furthermore, the dynamic behaviors of HOFs in response to external stimuli are also quite attractive. This dynamic behavior can significantly affect the properties of HOFs and even lead to many unpredictable results, which we will discuss in detail in this paper.

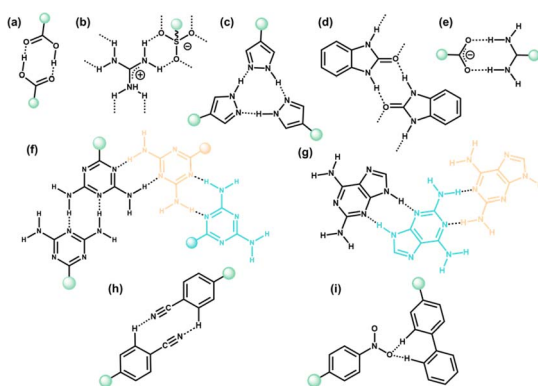


Fig. 1 Representative H-bonding motifs for the design of HOFs: (a) carboxyl dimer; (b) guanidinium-sulfonate; (c) pyrazole; (d) benzimidazolone; (e) amidinium-carboxylate; (f) 2,4-diaminotriazine; (g) 2,6-diaminopurine; (h) cyano group; (i) nitro group.

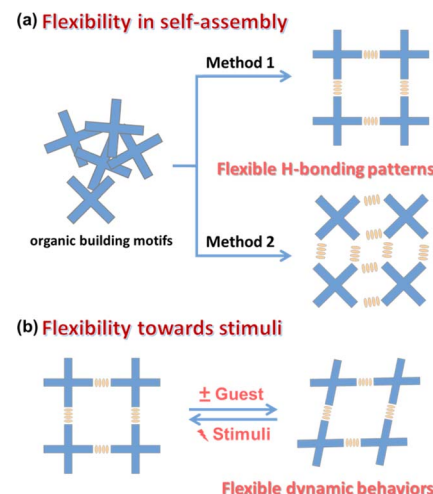


Fig. 2 The flexibility of HOFs in (a) the self-assembly process and (b) response to external stimuli.



Flexible HOFs have some obvious advantages: (1) more accessible flexible behaviors. Generally, the bonding energy of H-bonds is 10–40 kJ mol<sup>−1</sup>, much lower than the coordination bonds in MOFs (90–350 kJ mol<sup>−1</sup>) and the covalent bonds in COFs (300–600 kJ mol<sup>−1</sup>), making it easier for HOFs to exhibit a certain degree of structural flexibility and diversity;<sup>13</sup> (2) better reproducibility. The reversibility of H-bonds allows us to reconnect broken H-bonding units under certain conditions, enabling the original HOFs to recover and regenerate; (3) compared to MOFs, HOFs lack metal ions (or have a lower proportion of metal ions), resulting in lower density; however they exhibit higher structural diversity than COFs, combining the different advantages of both.

In this perspective, we aim to provide a unique viewpoint on discussing flexible HOFs. Rather than offering a comprehensive overview of all flexible HOFs, we will focus on discussing the

flexible behaviors of some representative flexible HOFs (Table 1) and their unique applications. Additionally, we will highlight the differences between flexible HOFs and other porous materials such as MOFs and COFs.

## 2. Different types of flexible behaviors

The flexibility of HOFs derives from the organic motifs as well as the weak bond strength and reversibility of the H-bond. We have so far obtained a lot of flexible HOFs, although in many cases, the fragility of the crystals makes it challenging to identify the structural changes where the flexible behavior occurs. Generally speaking, during the synthesis or in response to external stimuli, HOFs display four primary flexible features: pore size/shape changes, interpenetration/stacking manner, H-bond breaking/reconstruction, and local dynamic behavior (Fig. 3).

**Table 1** Selected representative flexible HOFs categorized into different flexible behaviors

Flexible behaviors		HOFs	Functionality	Ref.
Pore size/shape changes	Pore contraction/expansion	SOF-1 HOF-1 HOF-4 ZJU-HOF-1 HOF-40 HOF-FJU-8 Compound 2 HOF-5 HOF-7 8PN 2D-90 HOF-6 PET-HOF-1 PET-HOF-2 HOF-12 HOF-FJU-1 ZJU-HOF-8a LA-H-HexNet HOF-29 HOF-FJU-88 [(Bmib) <sub>3</sub> (H <sub>2</sub> O) <sub>12</sub> ] <sub>n</sub> HOF-30 PFC-71/72/73 Tri-PMDI-Br MEP-HOF FDU-HOF-3 PFC-77 PFC-78 PFC-79 HOF-FJU-2 HOF-NBDA BA-N BA-C HOF-30 H <sub>c</sub> OF-6 ABTPA-1 ABTPA-2 8PZ Cage-6-COOH	C <sub>2</sub> H <sub>2</sub> , CH <sub>4</sub> , CO <sub>2</sub> storage C <sub>2</sub> H <sub>2</sub> /C <sub>2</sub> H <sub>4</sub> separation C <sub>2</sub> H <sub>4</sub> /C <sub>2</sub> H <sub>6</sub> separation C <sub>2</sub> H <sub>6</sub> /C <sub>2</sub> H <sub>4</sub> separation Xe/Kr separation C <sub>2</sub> H <sub>2</sub> /CO <sub>2</sub> separation O <sub>2</sub> /Ar/N <sub>2</sub> separation CO <sub>2</sub> /CH <sub>4</sub> separation CO <sub>2</sub> /N <sub>2</sub> separation CO <sub>2</sub> /N <sub>2</sub> separation Molecular recognition Dynamic luminescence behavior Proton conductivity — — CO <sub>2</sub> /CH <sub>4</sub> separation C <sub>2</sub> H <sub>6</sub> /C <sub>2</sub> H <sub>4</sub> separation C <sub>3</sub> H <sub>6</sub> /C <sub>3</sub> H <sub>8</sub> separation C <sub>2</sub> H <sub>2</sub> /CO <sub>2</sub> separation <i>n</i> -C <sub>4</sub> H <sub>10</sub> /CH <sub>4</sub> separation Hydrocarbon sorption Molecular recognition CO <sub>2</sub> /C <sub>2</sub> H <sub>2</sub> separation — C <sub>3</sub> H <sub>6</sub> /C <sub>3</sub> H <sub>4</sub> separation Photocatalytic CO <sub>2</sub> reduction Bz/Cy separation Detection of nitrobenzene Ammonia capture — — — Acetone/methanol separation C <sub>2</sub> H <sub>6</sub> /C <sub>2</sub> H <sub>4</sub> separation Detection of acetone — C <sub>3</sub> H <sub>4</sub> /C <sub>3</sub> H <sub>6</sub> separation — — Programmable luminescence Vapor sorption	28 27 40 41 42 43 44 45 46 47 48 49 50 51 52 53 54 55 56 57 58 59 60 61 62 63 64 65 66 67 68 69 70 71 72 73
Interpenetration/stacking manner	Interpenetrated network			
H-bond breaking/reconstruction	Layer network sliding			
Local dynamic behavior				



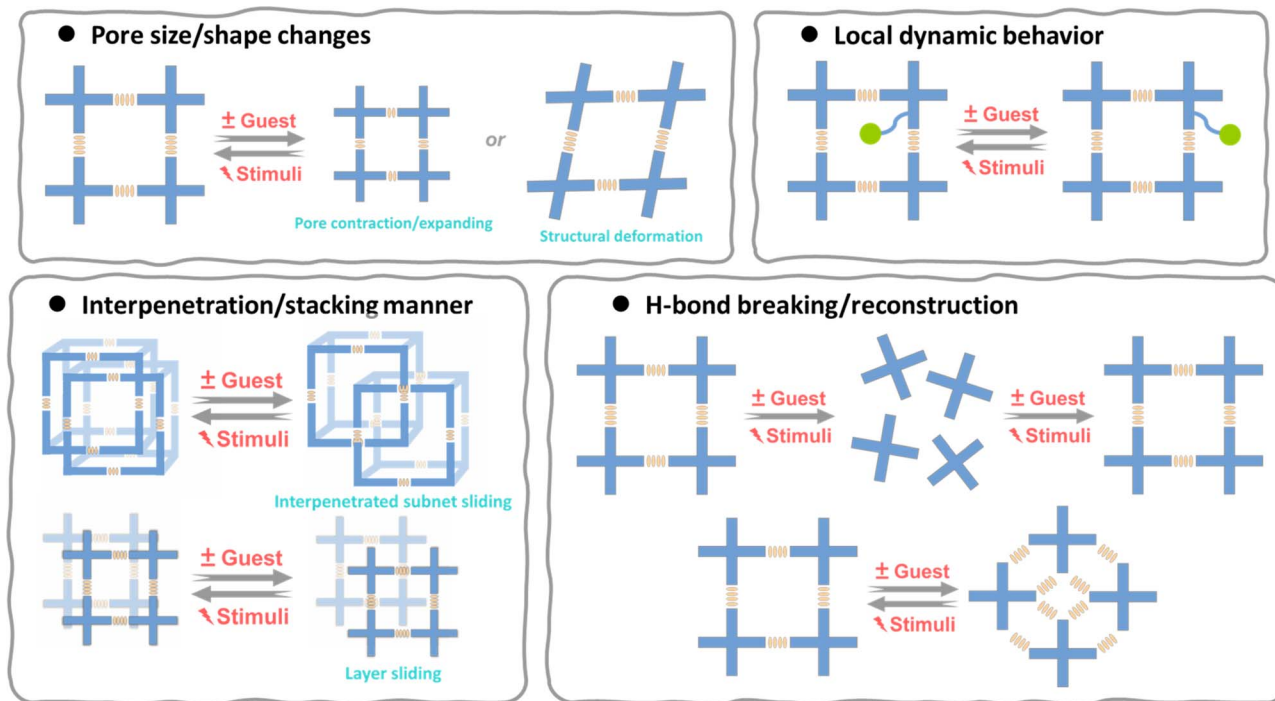


Fig. 3 Representative modes of different types of flexible behaviors for flexible HOFs.

## 2.1 Pore size/shape changes

The removal of guest molecules during the activation of flexible HOFs or under certain external stimuli often causes pore contraction/expansion, deformation of the structure, or both.<sup>27,28,40–48</sup>

**2.1.1 Pore contraction/expansion.** HOF-1 is a well-known HOF that first exhibited pore contraction/expansion behavior in gas adsorption.<sup>27</sup> This HOF is constructed from tetrakis(4-(2,4-diamino-1,3,5-triaryl)phenyl)methane *via* H-bonds between 2,4-diaminotriazine groups (Fig. 4a). The CO<sub>2</sub> adsorption at 196 K shows an obvious gate-opening effect at  $P/P_0 = 0.78$  as well as a large hysteretic desorption behavior, indicating that the pore structure of activated HOF-1a expanded with the increase of pressure to adsorb more guest molecules (Fig. 4b). Similar dynamic behavior was also observed for C<sub>2</sub>H<sub>2</sub> (Fig. 4c). PXRD confirms the reversible transformation between the guest-free HOF-1a and guest-loaded HOF-1 and exhibits reversible pore contraction/expansion behavior.

The process of pore expansion/contraction can be effectively characterized by *in situ* PXRD of the gas-loaded sample. In 2023, our group reported a flexible-robust HOF (HOF-FJU-8) derived from 4,4',4'',4'''-(pyrrolo[3,2-*b*]pyrrole-1,2,4,5-tetrayl)tetrabenzonitrile (DP-4CN) by employing a sticked-layer strategy.<sup>43</sup> Based on the CO<sub>2</sub> sorption isotherm at 196 K, the activated HOF-FJU-8a exhibits a stepwise adsorption isotherm, suggesting its framework flexibility and the existence of a gating effect. Furthermore, *in situ* PXRD of CO<sub>2</sub>-loaded HOF-FJU-8a at 196 K confirmed that with pressure increasing, Miller indices (102) shift slightly to the right, indicating a slight change in the structure. The pore-size distribution calculated from the CO<sub>2</sub> isotherm is also

slightly larger than the calculated one based on the single crystal structure due to the pore space expansion during the third step of the adsorption process.

**2.1.2 Structural deformation.** This flexible behavior is more common in MOFs since the flexibility originating from the metal nodes can easily cause changes in the coordination angle, leading to deformation of the channels, *e.g.*, the well-known MIL-53 (Cr and Al).<sup>74–76</sup> In HOFs, the structural deformation can come from the flexibility of the organic units or H-bonds. For example, in HOF-5, which is constructed from 4,4',4'',4'''-tetra(2,4-diamino-1,3,5-triazin-6-yl)tetraphenylethene (DAT), planar 4-connected organic building units can undergo notable structural deformation after full activation (Fig. 5).<sup>45</sup> The activated sample HOF-5a retains the same framework connectivity and topology but has less pore volume (41.1%) than HOF-5 (55.3%). The size of the channel in HOF-5 (22.5 × 34.7 Å) contracts to 17.8 × 36.5 Å in HOF-5a, which means that the shape of the channel is getting flattened.

Similar flexible behavior has been reported in other HOFs as well.<sup>46–48</sup> In 2021, Chi *et al.* reported the design and synthesis of a dynamic two-dimensional (2D) woven HOF.<sup>48</sup> The researchers were able to emulate a weaving craft by interlocking 1D strands through H-bonding, resulting in a 2D molecular woven network. Thus, the dynamic nature of the woven structure allows for reversible structural deformations in response to different solvents, as well as large-scale elasticity switching.

## 2.2 Interpenetration/stacking manner

It has been established that interpenetration is a crucial structural characteristic of porous materials because it can increase structural stability, endow the framework with flexibility, and



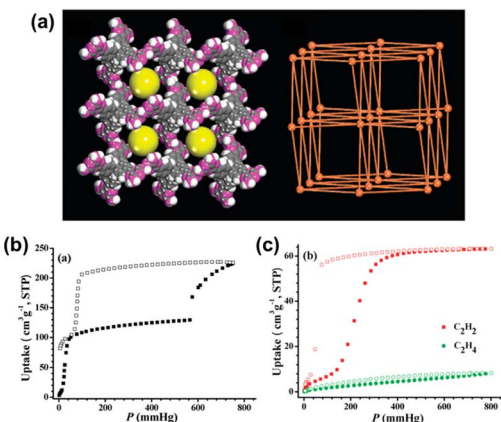


Fig. 4 (a) Single-crystal structure and topology of HOF-1; (b) CO<sub>2</sub> adsorption at 196 K; (c) C<sub>2</sub>H<sub>2</sub> and C<sub>2</sub>H<sub>4</sub> adsorption of HOF-1 at 298 K.<sup>27</sup>

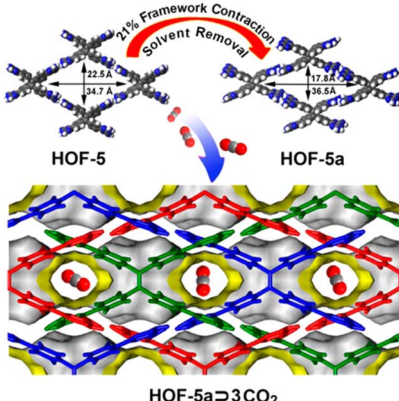


Fig. 5 Illustration of the structural deformation of HOF-5 and the arrangement of CO<sub>2</sub> molecules in the pores.<sup>45</sup>

allow for fine-tuning of the pore structure.<sup>77,78</sup> Therefore, realizing a controlled interpenetration design in HOFs can enhance functional diversity. Similarly, the layer-stacked 2D HOFs can also exhibit flexible behavior due to the relatively weak  $\pi$ - $\pi$  interactions between layers, resulting in sliding.

**2.2.1 Interpenetrated network.** In 2021, our group reported a microporous HOF-FJU-1, which is composed of 3,3',6,6'-tetra cyano-9,9'-bicarbazole *via* intermolecular H-bonding interactions.<sup>52</sup> Each carbazole unit is linked to four adjacent carbazoles by four pairs of C-N $\cdots$ H-C H-bonds with distances of 3.431–3.536 Å to form a **dia** topology (Fig. 6). HOF-FJU-1 exhibits a threefold-interpenetrated structure, with distinct offset  $\pi$ - $\pi$  interactions along the *a* axis. The pore windows in the channels have a size of about 3.4  $\times$  5.3 Å<sup>2</sup>, which is suitable for the separation of C<sub>2</sub>H<sub>4</sub>. This flexible HOF exhibits a gate-opening effect, where the opening pressure required for C<sub>2</sub>H<sub>4</sub> uptake varies with temperature. The *in situ* PXRD patterns of the CO<sub>2</sub> loaded sample at 195 K confirm the minor expansion of the pore window. Additionally, the interpenetrated network exhibits high stability even under various harsh conditions. A similar phenomenon can also be found in other cases.<sup>49–51,53</sup>

**2.2.2 Layer network sliding.** The flexible behavior of 2D HOFs has also been observed in single-crystal structures. In 2022, our group reported an adaptive HOF, HOF-29, based on 4,4',4'',4'''-(porphyrin-5,10,15,20-tetrayl)tetra benzonitrile (PTTBN).<sup>57</sup> Each PTTBN unit is connected with four adjacent units *via* four pairs of intermolecular C-H $\cdots$ NC H-bonds, resulting in a 2D **sql** net. Different layers were packed in an AA stacking pattern through multiple H-bonding and  $\pi$ - $\pi$  stacking interactions (Fig. 7a and b). HOF-29 exhibited a single-crystal-to-single-crystal transformation from the as-synthesized AA stacking phase to another AB stacking phase after adsorbing pX molecules by sliding the 2D layers and the local distortion of the ligand (Fig. 7c and d) realized the exclusive recognition of pX over mX, oX and EB.

In some other studies, the flexibility of 2D HOFs has already been applied in the field of gas separation.<sup>56,58</sup> In 2023, Zhang *et al.* reported a CO<sub>2</sub>-selective HOF-FJU-88 from 2,4,6-tri(1H-pyrazol-4-yl)pyridine (PYTPZ) building units.<sup>58</sup> HOF-FJU-88 consists of a 2D H-bonded layer formed from PYTPZ molecules. Each layer is further connected by  $\pi$ - $\pi$  interactions between pyridine and pyrazole groups. During the activation process, PXRD indicates a partial loss of crystallinity due to the sliding of the 2D layers. The CO<sub>2</sub> adsorption isotherm also exhibits a significant gate-opening effect, demonstrating the dynamic framework nature of HOF-FJU-88.

### 2.3 H-bond breaking/reconstruction

The reversibility of the H-bonds offers HOFs a unique type of flexibility; that is, HOFs are able to return to their initial states if the structures collapse following a stimulus response, which includes physical stimuli (pressure, temperature, guest molecules, *etc.*) and chemical stimuli (acid, base, corrosive gases, *etc.*).<sup>59–69</sup> Or, sometimes, the H-bonding patterns will just be reorganized without losing the framework crystallinity, thus leading to a structural transformation. For example, the ethanol-bridged carboxyl dimers in HOF-30 reported by Wang *et al.* have exhibited reversible structural transformations with the removal of ethanol during the activation process or soaking in the solvent again.<sup>69</sup>

In 2024, Li *et al.* reported a microporous HOF, FDU-HOF-3, for ammonia (NH<sub>3</sub>) capture. This HOF is developed from 3,3',3'',3'''-(pyrene-1,3,6,8-tetrayl)tetra benzoic acid (H<sub>4</sub>PTTB) organic units.<sup>64</sup> In the structure, each H<sub>4</sub>PTTB building block was connected to four adjacent units *via* intermolecular H-bonds, along with intermolecular  $\pi$ - $\pi$  stacking interactions, forming a three-dimensional (3D) network with **sql** topology (Fig. 8a). Interestingly, FDU-HOF-3 will lose its crystallinity after NH<sub>3</sub> adsorption. However, after regeneration by heating and degassing, the regenerated HOFs return to the crystalline phase again. Further research demonstrated that the COOH-NH<sub>3</sub> acid-base interactions, along with the breaking and regeneration of COOH-COOH H-bonds, contributed to this HOF's self-healing behavior (Fig. 8b).

Another typical example was reported in 2023 by Wu *et al.* HOF-NBDA(DMA) was constructed from 4',4'',4'''-nitrilotris([1,1'-biphenyl]-3,5-dicarboxylic acid) (H<sub>6</sub>NBDA).<sup>67</sup> Each organic unit is



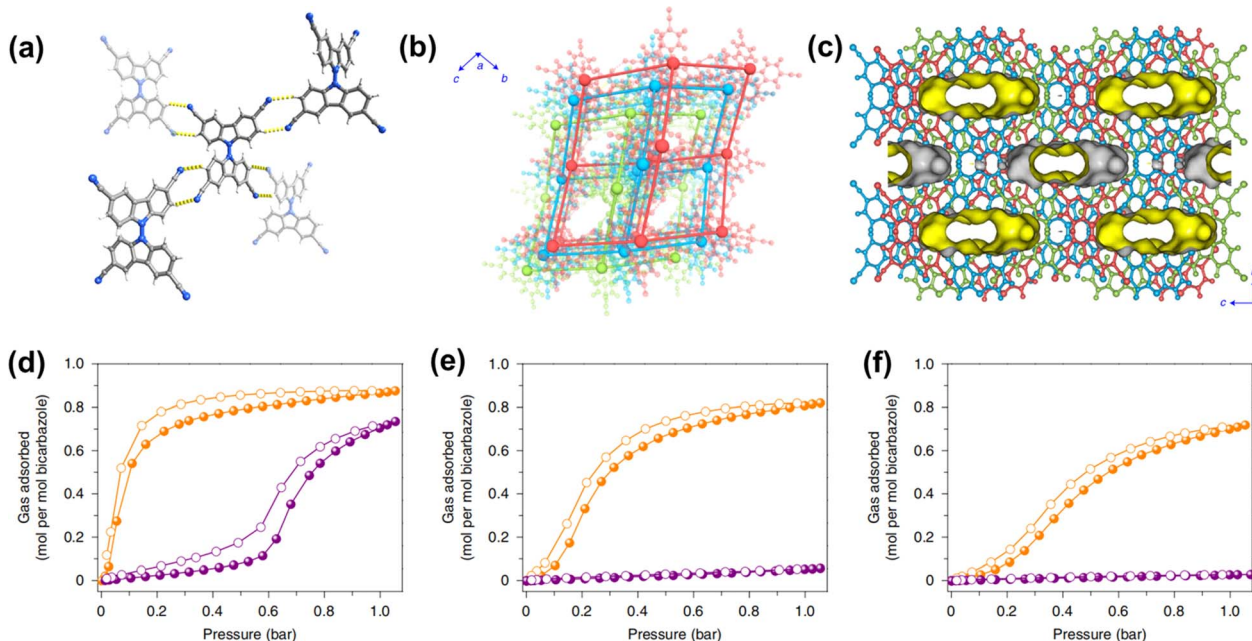


Fig. 6 (a) The intermolecular H-bonding interactions between bicarbazole units; (b) the threefold-interpenetrated dia net; (c) pore channels along the [100] direction; (d–f) gas adsorption isotherms for C<sub>2</sub>H<sub>4</sub> (orange) and C<sub>2</sub>H<sub>6</sub> (purple) at 298 K, 318 K and 333 K, respectively.<sup>52</sup>

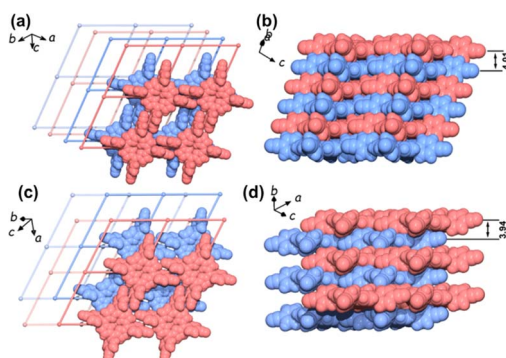


Fig. 7 The AA stacking pattern of HOF-29 viewed perpendicularly (a) and side views (b); the AB stacking pattern of HOF-29-pX viewed perpendicularly (c) and side views (d).<sup>57</sup>

connected to three adjacent H<sub>5</sub>NBDA units through six sets of intermolecular H-bonds to form a 2D honeycomb-like layer. It is worth noting that there are two types of H-bonds in HOF-NBDA(DMA). As shown in Fig. 9, H-1 is the classic carboxyl dimer that forms a pair of parallel H-bonds. However, in H-2, one carboxyl group was deprotonated, and thus further connected to another DMA cation *via* a N–H···O H-bond to balance the charge, resulting in a relatively low symmetry of the monoclinic *P*1 space group. However, upon activation, HOF-NBDA(DMA) transformed into another structure, HOF-NBDA. The single-crystal structure revealed that only H-1 type H-bonds remain; all the carboxyl groups are not deprotonated. The resulting HOF-NBDA exhibited a relatively high symmetry of the orthorhombic *Fddd* space group.

In 2023, Zhao *et al.* reported a very interesting study. Two different macrocyclic molecules, trimeric pyromellitic diimide (Tri-PMDI) and Tri-PMDI-Br, are synthesized and crystallized

into two distinct structures (Fig. 10).<sup>62</sup> In Tri-PMDI, H-bond interactions between the Ph–H and the O=C hold the molecules together and finally lead to the formation of PMC-Tri-PMDI (PMC, porous molecular crystals). For Tri-PMDI-Br, an unusual H-bond forms between C(sp<sup>3</sup>)–H from the cyclohexane and O=C, leading to the formation of HOF-Tri-PMDI-Br. The obtained HOF-Tri-PMDI-Br can simultaneously exhibit robustness and flexibility. The structural flexibility enables a reversible transformation between non-crystalline and crystalline phases by introducing or removing some specific solvent molecules, which act as a “key” to control the crystallinity. The single crystal structure of *n*-hexane@HOF-Tri-PMDI-Br has shown that *n*-hexane could easily go through the smaller pore of HOF-Tri-PMDI-Br and form H-bonds with cyclohexane linkages. Interestingly, only the solvent molecules with short chains, such as *n*-pentane and *n*-hexane, have the effect of crystallinity recovery. From this example, we can see the unexpected impact that a cleverly designed organic building block can have on the properties of a flexible HOF.

Recently, Zhang *et al.* reported a multifunctional HOF (HOF-FJU-2) using a tetrabenzaldehyde molecule, 4,4',4'',4'''-(9H-carbazole-1,3,6,8-tetrayl) tetrabenzaldehyde (CTBA), with a carbazole N–H binding site (Fig. 11).<sup>66</sup> This D–π–A type molecule has been confirmed to be able to construct flexible and/or flexible-robust HOFs for unprecedented functions. In this work, HOF-FJU-2 can be crystallized from different solvents. HOF-FJU-2 exhibits a 3D framework where CTBA molecules form π-stacking rod dimers. These dimers connect *via* H-bonds (C–H···O) and π–π interactions between aldehyde and carbazole groups, leading to the formation of larger π-stacking rod structures. The framework extends further through interactions between adjacent rod dimers, facilitated by C–H···O=C H-bonds. Interestingly, the

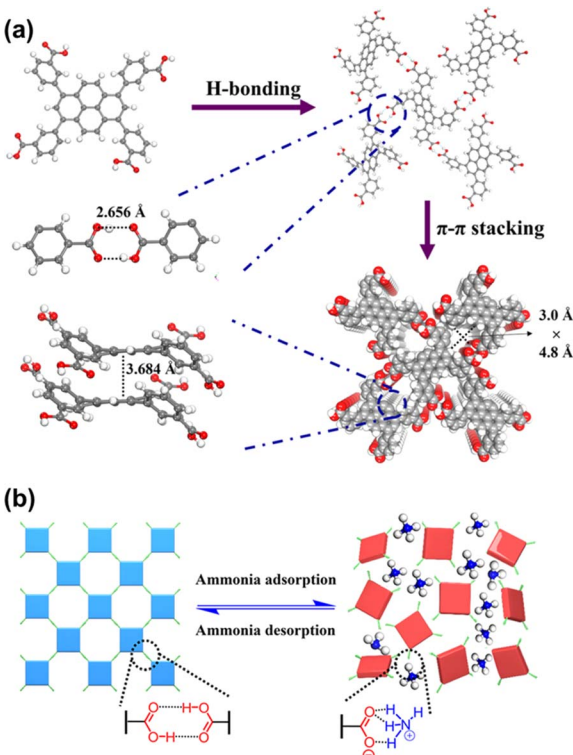


Fig. 8 (a) Crystal structures of FDU-HOF-3; (b) schematic illustration of the self-healing effect of FDU-HOF-3 before and after  $\text{NH}_3$  capture.<sup>64</sup>

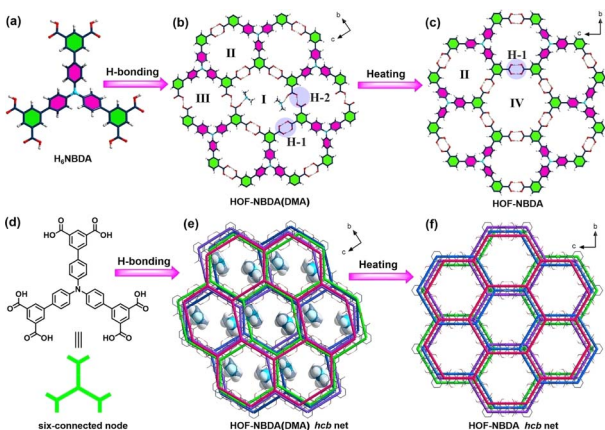


Fig. 9 (a) The structure of  $\text{H}_6\text{NBDA}$ ; (b and c) representation of the reorganization of H-bond dimers upon heating; (d) scheme of  $\text{H}_6\text{NBDA}$  and the six-connected node; (e and f) the transformation of layered frameworks before and after heating.<sup>67</sup>

activation of HOF-FJU-2 will result in a single-crystal-to-single-crystal (SCSC) transformation to a closed framework HOF-FJU-2a. However, when soaked in acetone or exposed to acetone vapor, the yellow HOF-FJU-2a crystals can be facilely transformed back into the white porous HOF-FJU-2, exhibiting flexibility in structure. Unlike HOF-FJU-1, the H-bonds formed between the CTBA molecules are not in pairs like in HOF-FJU-1, thus further increasing the local flexibility and leading to structural transformation during the activation process. However, the overall

stronger intermolecular interactions still maintain the stability of HOF-FJU-2, allowing this flexible HOF to exhibit related properties while maintaining crystallinity.

#### 2.4 Local dynamic behavior

The concept of local dynamics highlights the local motions throughout the entire framework in contrast to the behavior of global dynamics. It has been well established that modifying dangling groups on organic ligands in MOFs can lead to flexible behavior, even though the framework may not exhibit significant flexibility. The dangling groups can be small groups or complex interlocking supramolecular structures. Similarly, in HOFs, local flexibility in the organic units can bring about significant dynamic behavior, and this effect can either affect the properties or bring about a structural change. In addition, the rotation of the covalent bonds in the organic unit also brings about flexibility and results in structural diversity.<sup>71-73</sup>

In 2023, Chi *et al.* reported a flexible HOF, 8PZ, with local dynamics for adaptive guest accommodation through incorporating soft ethyl-ester chains.<sup>72</sup> 8PZ was developed from a flexible building block tetraethyl 4',4'',4''',4''''(ethene-1,1,2,2-tetrayl)tetrakis([1,1'-biphenyl]-4-carboxylate) (TPE-4PZ), which includes four identical soft ethyl-ester chains. 8PZ has been confirmed to have significant local dynamics in response to solvents and temperature changes, especially the in-plane and out-of-plane motions of terminal carbon atoms, leading to an effective approach to regulating the pore sizes. In 2023, Little *et al.* reported a flexible oxygen-bridged prismatic organic cage molecule, Cage-6-COOH, which has three pillars that exhibit rotational motion like a hinge in the solid state (Fig. 12).<sup>73</sup> This organic building unit can form a series of flexible HOFs by crystallizing in different solvents. CageHOF-2 $\alpha$  was crystallized from the THF/CH<sub>3</sub>CN solution, and each Cage-6-COOH molecule was connected to six neighboring Cage-6-COOH molecules *via* H-bonds between directional carboxylic acid dimers with distances of 2.58–2.59 Å. Although CageHOF-2 $\alpha$  shows an **acs** topology, it is nonporous. Another CageHOF-2 $\beta$  was crystallized from ethanol with similar H-bonding patterns. However, in CageHOF-2 $\beta$ , the H-bond building units are not all planar, and the aromatic pillars have profoundly different orientations. CageHOF-2 $\beta$  exhibited good thermal stability and a BET surface area of 458 m<sup>2</sup> g<sup>-1</sup>. Furthermore, another five HOFs are found with different dihedral angles between the pillars varying from 90° to 157°. The flexibility of Cage-6-COOH allows this molecule to rapidly transform from a low-crystallinity solid into CageHOF-2 $\alpha$  and CageHOF-2 $\beta$  under mild conditions simply by using acetonitrile or ethanol vapor, respectively. This work highlights the potential of flexible organic cage hinges in the design and synthesis of flexible HOFs with tunable properties.

### 3. Diverse applications for flexible HOFs

Flexible HOFs stand out because of their inherent flexibility, offering a wide range of potential applications. Although still



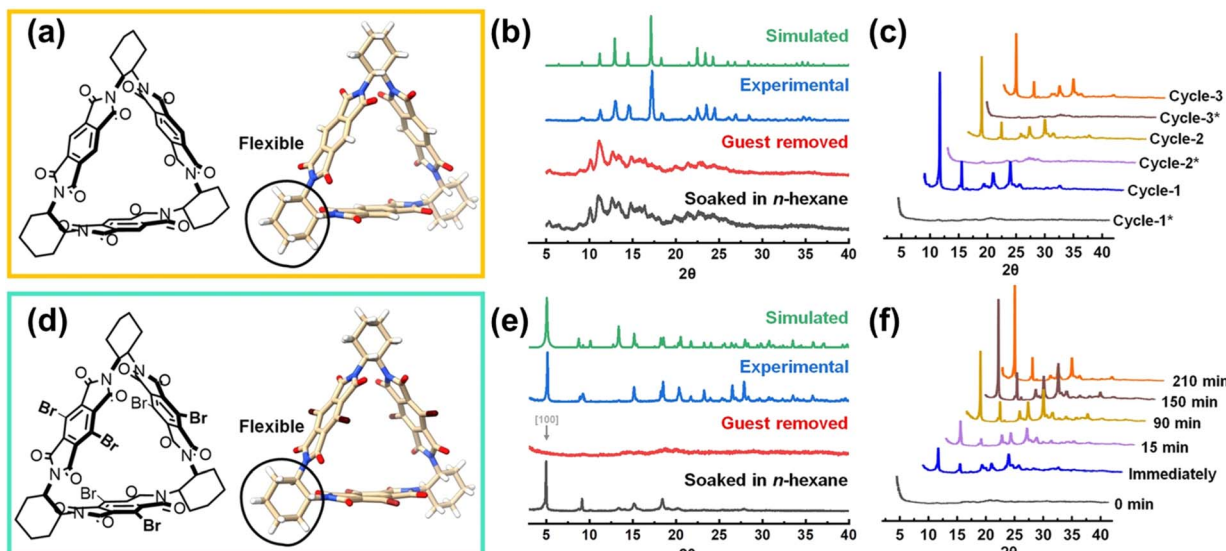


Fig. 10 (a and d) The chemical structures of Tri-PMDI and Tri-PMDI-Br, respectively; (b) PXRD patterns of PMC-Tri-PMDI; (c) PXRD patterns of HOF-Tri-PMDI-Br after removal and resoaking in *n*-hexane three times; (e) PXRD patterns of HOF-Tri-PMDI-Br; (f) PXRD patterns of HOF-Tri-PMDI-Br soaked in *n*-hexane for different intervals of time.<sup>62</sup>

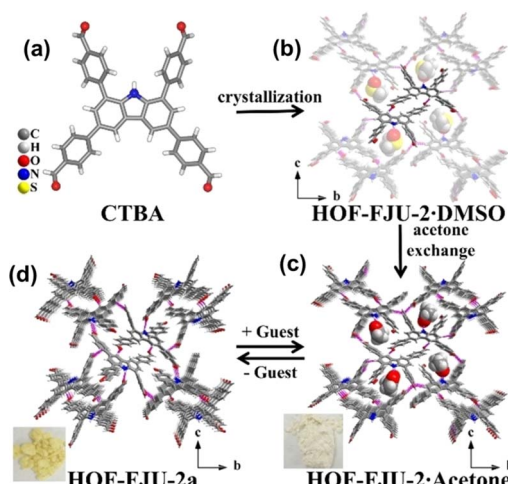


Fig. 11 (a) The tetrabenzaldehyde molecule CTBA; (b) structure of HOF-FJU-2·DMSO; (c) HOF-FJU-2·Acetone; (d) reversible SCSC transformation after guest removal to nonporous HOF-FJU-2a.<sup>66</sup>

relatively short in development compared to flexible MOFs and COFs, flexible HOFs have demonstrated their unique advantages in gas storage/separation, molecular recognition, biomedicine, heterogeneous catalysis, chemical sensing, and other areas. Their outstanding flexibility, along with the reversibility of H-bonding, allows them to be synthesized from a diverse range of building blocks, enabling mild synthetic reactions, excellent solution processability, easy repair, easy regeneration, and recyclability.

### 3.1 Gas storage/separation

The ability of flexible HOFs to adjust their structure dynamically when facing changes in temperature, pressure, or guest

molecule adsorption offers excellent potential for gas storage/separation. This dynamic response allows for interesting changes in pore sizes and shapes to effectively adsorb and separate specific gas molecules.<sup>27,28,38,40–43,45,46,49,51–54,58,60,64,66,67,79–89</sup> In addition, the recyclability of HOFs reduces the cost. The dynamic behavior of flexible HOFs in gas adsorption makes the research more complex than that of other rigid porous materials. Therefore, many *in situ* characterization methods have been used in recent years to help us better understand this behavior.

Early in 2010, Schröder *et al.* reported the gas adsorption of SOF-1, which demonstrated impressive adsorption capabilities for CH<sub>4</sub> (106 cm<sup>3</sup> g<sup>-1</sup>, 10 bar, and 195 K), C<sub>2</sub>H<sub>2</sub> (124 cm<sup>3</sup> g<sup>-1</sup>, 1 bar, and 195 K), and CO<sub>2</sub> (69 cm<sup>3</sup> g<sup>-1</sup>, 16 bar, and 298 K).<sup>28</sup> Most notably, the activated SOF-1a demonstrated a flexible response to temperature increases from 77 K to 125 K, with a significant increase in N<sub>2</sub> adsorption capacity, indicating a certain framework flexibility. Such a flexible behavior appears to be more pronounced in HOF-1 and is applied for the first time in the field of gas separation.<sup>27</sup> As described above, HOF-1 exhibited a significant gate-opening effect on C<sub>2</sub>H<sub>2</sub>. The adsorption isotherm of C<sub>2</sub>H<sub>2</sub> showed a sudden increase around 200 mmHg, with a final adsorption capacity of 63.2 cm<sup>3</sup> g<sup>-1</sup> (at 800 mmHg and 273 K). Meanwhile for C<sub>2</sub>H<sub>4</sub> it only adsorbed 8.3 cm<sup>3</sup> g<sup>-1</sup> under the same conditions, thus leading to a highly selective adsorptive separation of C<sub>2</sub>H<sub>2</sub> and C<sub>2</sub>H<sub>4</sub> at ambient temperature. The subsequently reported HOF-5 also exhibits high porosity and CO<sub>2</sub> adsorption capacity.

After these early studies, a large number of flexible HOFs have been reported for gas adsorption/separation. As mentioned above, HOF-FJU-1 showed a clear gate-opening effect due to the interpenetrated framework, and the experimental results showed that the adsorption capacity for C<sub>2</sub>H<sub>4</sub> was 47 cm<sup>3</sup> g<sup>-1</sup> at 298 K and 1 bar, while for C<sub>2</sub>H<sub>6</sub> it was very

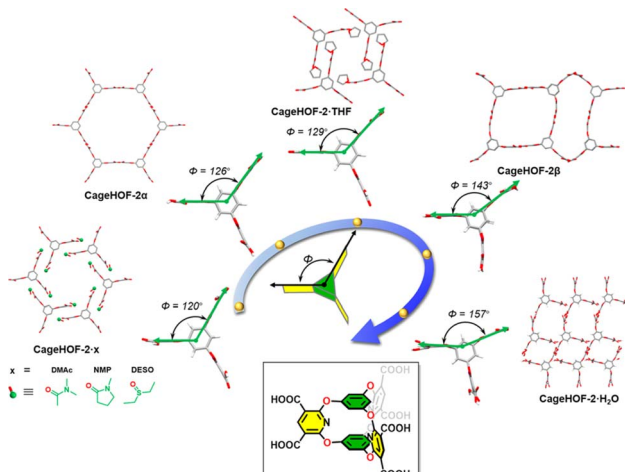


Fig. 12 Schematic illustration of the dihedral angles of the pillar ring changes from  $90^\circ$  to  $157^\circ$  in Cage-6-COOH based structures.<sup>73</sup>

low.<sup>52</sup> In addition, with the increase in temperature, the adsorption capacity for  $C_2H_6$  will further decrease. Breakthrough experiments confirmed the high selectivity of HOF-FJU-1 for  $C_2H_4$  with a purity of 99.1% at 333 K. It is worth mentioning that HOF-FJU-1 exhibits stability under various harsh conditions and can be easily processed into different forms for gas separation. Interestingly, theoretical simulation

shows that neither  $C_2H_4$  nor  $C_2H_6$  molecules can diffuse into HOF-FJU-1 without considering the flexibility of the framework, but the distribution of  $C_2H_4$  in the pore is clearly observed by single crystal X-ray diffraction, which fully demonstrates the key role of flexibility in this adsorption process. However, in another study, instead of showing the same flexibility towards smaller gas molecules ( $C_2H_2$  and  $CO_2$ ), HOF-FJU-1 achieves the high sieving effect of  $C_2H_2/CO_2$ .<sup>54</sup> Therefore, such an interesting robust-flexible HOF exhibited completely different adsorption behaviors with different adsorption guests, showing the remarkable versatility of flexible HOFs.

Very recently, Li *et al.* reported a carboxyl-based HOF, ZJU-HOF-8, with flexible-robust porosity for natural gas purification.<sup>55</sup> ZJU-HOF-8 is constructed from 2,3,5,6-tetrakis(4-carboxyphenyl)-pyrazine ( $H_4TCPZ$ ) organic units *via* intermolecular C-H $\cdots$ N, C-H $\cdots$ O and C-H $\cdots$  $\pi$  interactions (Fig. 13a). ZJU-HOF-8 exhibits a unique four-fold interpenetrated subnetwork. Gas sorption and X-ray diffraction studies confirm that the activated ZJU-HOF-8a exhibits a significant structural contraction, showing selective pore-pocket opening by certain gas molecules. This selective opening leads to higher uptakes and enhanced selectivities for  $C_3H_8$  and  $n-C_4H_{10}$  over  $C_2H_6$  and  $CH_4$ , highlighting the potential for designing flexible-robust HOFs for improved gas separation (Fig. 13b-d).

The potential application of flexible HOFs in gas adsorption/separation is actually more widespread. The renewability of

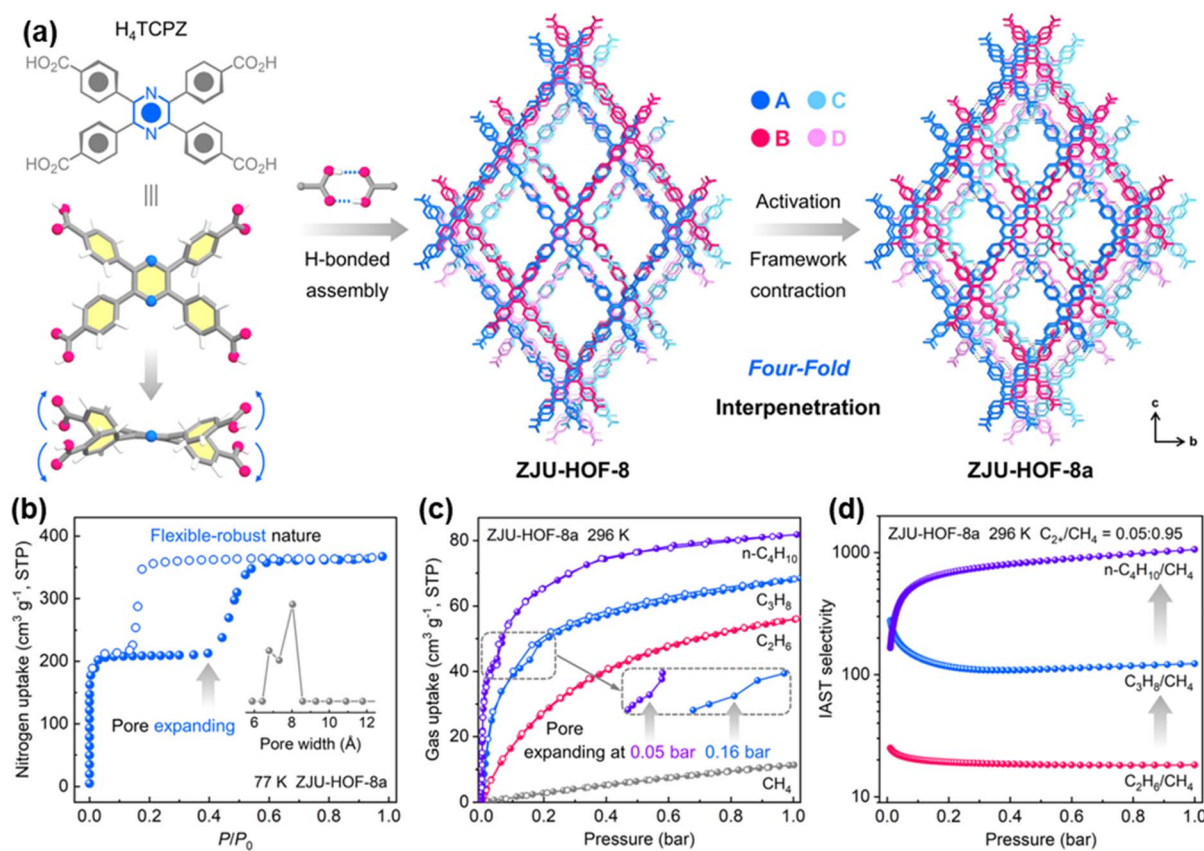


Fig. 13 (a) Single-crystal structure of ZJU-HOF-8 and the structural transformation with framework contraction upon activation; (b)  $N_2$  adsorption of ZJU-HOF-8a at 77 K; (c) different gas adsorption at 296 K; (d) IAST selectivities of ZJU-HOF-8a at 296 K.<sup>55</sup>



HOFs, in particular, provides this material with a unique economic advantage. Their lower density, on the other hand, allows for a better balance of volumetric and gravimetric uptake, which is also an important aspect in this field.<sup>90</sup> Flexible HOFs, in general, can exhibit more unpredictable dynamic behaviors, allowing them to deal with some difficult separation systems and establish a new class of energy-saving and environmentally friendly physical adsorbents.

### 3.2 Molecular recognition

In molecular recognition applications, flexible HOFs can precisely accommodate guest molecules within their pores through dynamic structural changes.<sup>47,57,86,91</sup> This attribute enables selective binding and recognition of target molecules, which is crucial for sensors, drug delivery systems, and chemical sensing applications. By adjusting the framework's flexibility, researchers can enhance the specificity and efficiency of molecular recognition processes, paving the way for advanced sensing technologies and targeted therapeutics.

Ward *et al.* have reported a series of host frameworks based on guanidinium cations and interchangeable organosulfonate anions, which exhibited impressive flexible behaviors. In these compounds, the guanidinium molecules are connected to sulfonate *via* N-H···O-S H-bonds, forming a 2D quasi-hexagonal H-bonding network.<sup>25,92</sup> Different types of organosulfonate molecules will further connect the layer, resulting in diverse structures. The flexibility of the H-bonded network allows these compounds to adapt to changes in the steric requirements of guest molecules that occupy the channels. The typical example reported in 1997 described a case of HOF, (G)<sub>2</sub>(BPDS) based on guanidinium (G) and 4,4'-biphenyldisulfonate (BPDS).<sup>25</sup> Single-crystal diffraction results show that each BPDS molecule is connected to six G molecules *via* N-H···O-S H-bonding, resulting in a pillared structure. A variety of flexible response forms are observed, including (1) N-H···O-S H-bonding rotations; (2) twisted C-C bonding in BPDS molecules; (3) rotations of the C-S bonding in the BPDS molecules;

(4) different H-bonding patterns in the guanidinium-sulfonate layer structure; (5) selection of "bilayer" *versus* "brick" stacking patterns. Guanidinium is capable of changing its pore structure to accommodate various monosubstituted benzene guests and disubstituted isomers, revealing host-guest interactions.

Another interesting recent study was reported in 2019. Chi *et al.* found an exceptionally flexible HOF, 8 PN, which exhibited permanent porosity derived from 1,1,2,2-tetrakis(4'-nitro-[1,1'-biphenyl]-4 yl)ethane.<sup>47</sup> 8 PN exhibits unprecedented flexibility, allowing for the regulation of pore volume in HOFs through the control of molecular assembly and conformation. Nine different single crystals of 8 PN achieved a pore volume adjustment ranging from 89.4 Å<sup>3</sup> to 1816.0 Å<sup>3</sup> (Fig. 14). Moreover, the pore volume adjustment enables multimodal reversible structural transformations in response to various external stimuli, including guest molecules, temperature variations, and mechanical pressure changes. Flexible frameworks can accommodate guest molecules of different sizes, thereby yielding five high-quality co-crystals, further indicating the potential application prospects of flexible 8PN in adaptively regulating pore structures.

In 2023, Xue *et al.* reported a flexible luminescent HOF for the separation of benzene and cyclohexane.<sup>93</sup> The researchers designed and synthesized a nonplanar phenothiazine derivative with three cyano moieties (PTTCN) as the functional crystal (Fig. 15). Two different forms of PTTCN crystals, ax form and eq form, have different fluorescence colors. The ax form crystals were found to selectively adsorb benzene through an SCSC transformation. However, the purity of the separated benzene from a benzene/cyclohexane equimolar mixture was relatively low at 79.6%. On the other hand, the eq form of PTTCN molecules co-assembled with benzene to construct an HOF (X-HOF-4) with S-type solvent channels and yellow-green fluorescence. This flexible HOF exhibited a strong preference for aromatic benzene over cyclohexane. The researchers discovered that the framework could release benzene to form a nonporous guest-

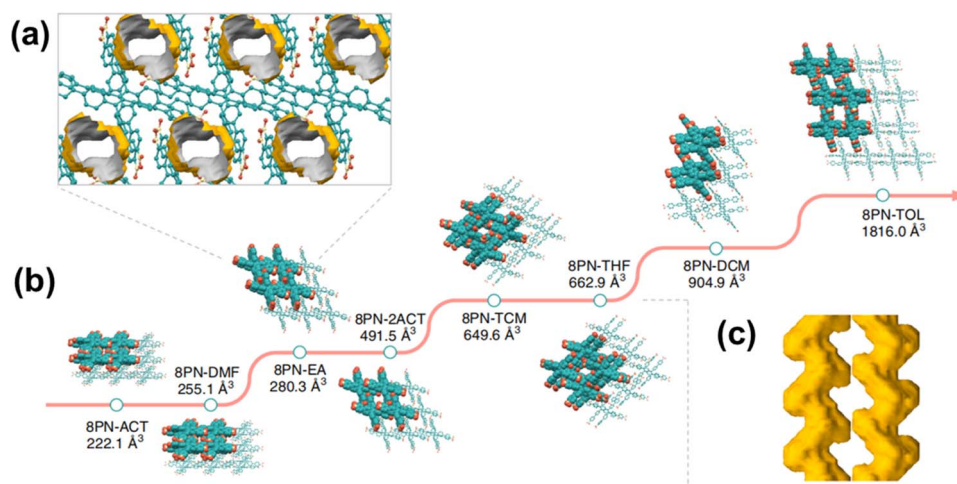


Fig. 14 (a) Packing model of 8PN-EA in the [010] direction, with the solvent-accessible void space; (b) single-crystal X-ray structures of eight 8 PN frameworks with varying void space; (c) S-shaped channel surface of 8PN-THF.<sup>47</sup>



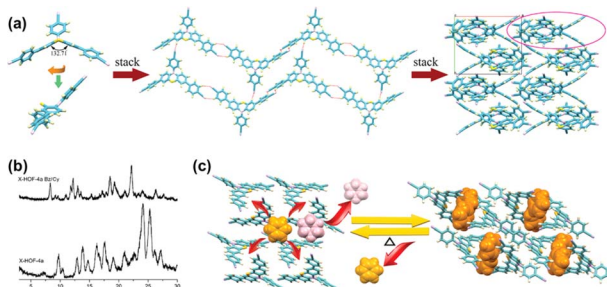


Fig. 15 (a) Assembling of PTTCN molecules (left) to a 2D H-bonded framework with pores (middle), and intermolecular stacking in a  $2 \times 2$  cell (right); (b) PXRD patterns; (c) schematic representation of the separation for benzene/cyclohexane.<sup>93</sup>

free crystal under heating. This nonporous crystal could selectively reabsorb benzene from the benzene/cyclohexane mixture, allowing for the recovery of the original framework. The purity of the reabsorbed benzene reached approximately 96.5%. This work addressed the challenge of separating benzene and cyclohexane by designing a flexible luminescent HOF with selective adsorption and release properties.

### 3.3 Sensing

HOFs have demonstrated significant promise in the fields of multiple stimulus-response and intelligent optics because of their modular building units and flexible frameworks. As a multifunctional luminescent framework material with both luminescent and porosity properties, it has a broad application prospect in the field of sensing.<sup>63,68,72,94-102</sup>

A novel triaryl formamidine salt containing two isomers (BA-C and BA-N) was reported by Lin *et al.*<sup>68</sup> These two isomers can be recrystallized in different solvents to form two different HOFs, and it was found that the removal of acetone from the lattice of BA-C by grinding or heating could lead to the conversion of BA-C to BA-N, and in turn, exposing to acetone vapor or cooling at 77 K could lead to the conversion of BA-N to BA-C, thus realizing the reversibility of the conversion of BA-N and BA-C, and showing the flexibility of these HOFs (Fig. 16). The flexible behavior of this anionic HOF enables dynamic switching of multiple luminescence behaviors, including prompt fluorescence, TADF, and phosphorescence. As a result, this HOF can be used for highly sensitive and specific sensing of acetone with an ultra-low detection limit of 66.74 ppm.

There are many similar examples of utilizing the flexible behavior of HOFs to achieve fine-tuning of optical properties, such as the previously mentioned 8PZ, where soft ethyl-ester chains bring adaptability to different guest molecules, and endow it with programmable temperature-dependent luminescence behaviors.<sup>72</sup> In another case, Cong *et al.* reported a novel polycatenated HOF MEP-HOF, which is composed of fluorenylidene-aza[1<sub>6</sub>]cyclophane (FLAC).<sup>63</sup> This HOF exhibits dynamic reversible transformation in crystallinity during guest removal/adsorption and also exhibits sensitive detection of nitrobenzene. In 2021, Xue *et al.* investigated the influence of guest molecules on the photoluminescence and force-stimuli

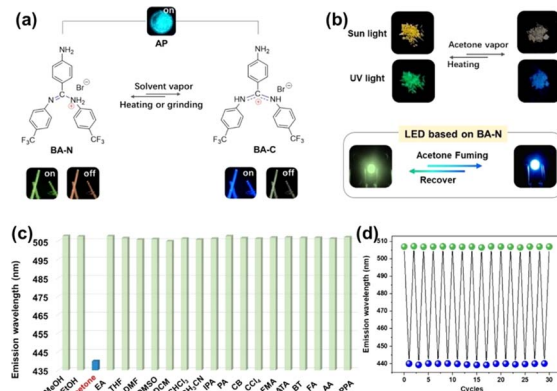


Fig. 16 (a) Tautomerism of BA-N and BA-C; (b) images showing reversible switching between BA-N and BA-C ( $\lambda_{\text{ex}} = 365 \text{ nm}$ ), as well as LED light-emitting images before and after acetone fumigation; (c) histogram of the prompt emission peaks of BA-N following fumigation; (d) repeatability of luminescence color switching when stimulated with acetone vapor and heated.<sup>68</sup>

response of X-HOF-1.<sup>102</sup> The research demonstrated that the mechanofluorochromic HOF materials could be regenerated through recrystallization and adsorbing the guest and highlighted the potential of guest molecules in regulating the properties and functions of flexible HOFs.

### 3.4 Biomedical applications

HOFs are a promising material for biomedical applications due to their excellent biocompatibility and low toxicity. One of the most significant advantages of flexible HOFs is their ability to adaptively accommodate a variety of guest molecules, enabling reversible guest encapsulation and controlled release in response to mild stimuli. Thus, flexible HOFs offer promising opportunities for targeted drug delivery, antimicrobial therapies, and anticancer treatments, providing innovative solutions to biomedical challenges.<sup>103-106</sup>

A very typical example of a drug carrier is PFC-1, which is a photoactive HOF for synergistic chemo-photodynamic therapy.<sup>107</sup> Subsequently, much work has been reported in this field, and flexible HOFs act as carriers or shells to protect or transport biomedical molecules. In 2022, Ouyang *et al.* reported a case where by encapsulating cytochrome c (Cyt c), a heme-containing enzyme, within HOF-101, they could create a biomimetic system that allowed for non-native biocatalytic activity (Fig. 17).<sup>108</sup> The results of the experiment demonstrate that the H-bonded nano-biointerface between encapsulated Cyt c and the HOF cage induces Cyt c to alter its native conformation. This work demonstrates the synergistic relationship between Cyt c and HOFs in terms of structural flexibility.

In recent years, more and more scientists have applied flexible HOFs in the biomedical field. In 2022, Qu *et al.* reported the development of a novel strategy for the encapsulation and transplantation of neural stem cells (NSCs) using a HOF as a protective shell (Fig. 18).<sup>109</sup> The HOF-based cell protectors effectively shielded the NSCs from physical and chemical stressors. They were degradable under near-infrared II (NIR-II)

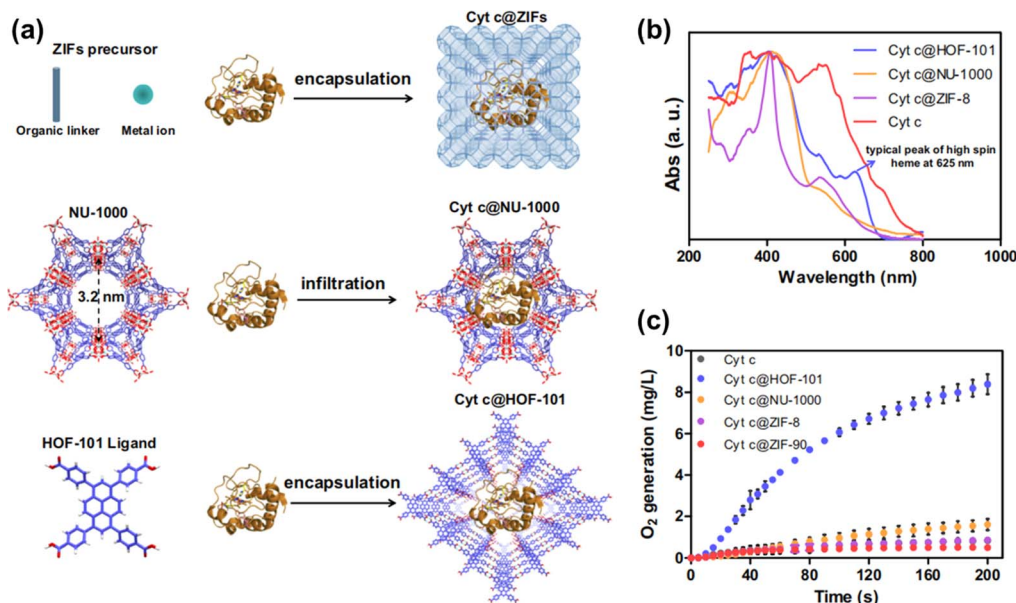


Fig. 17 (a) Schematic illustration of the synthesis of Cyt c@ZIFs, Cyt c@NU-1000, and Cyt c@HOF-101; (b) normalized UV-Vis DRS; (c) CAT-like bioactivities of Cyt c@ZIFs, Cyt c@NU-1000 and Cyt c@HOF-101.<sup>108</sup>

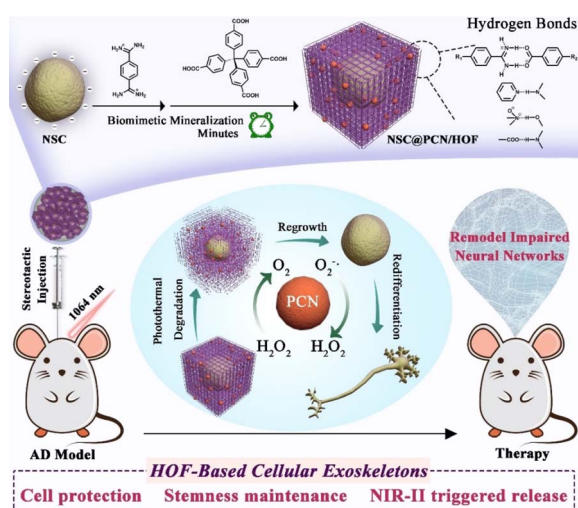


Fig. 18 A schematic representation of the construction and removal of HOF shells on individual NSCs, as well as the process for remodeling impaired neural networks.<sup>109</sup>

laser irradiation, allowing for controlled release of the encapsulated NSCs, which benefited from the weak bonding strength of HOFs. The transplantation of NSC@PCN/RA/HOF and subsequent NIR-II laser irradiation resulted in significant improvement in cognitive function in AD mice, as demonstrated by the Morris water maze test. The treated mice showed shorter escape latency, increased time spent in the target quadrant, and improved swimming speed compared to the control groups. Overall, this research demonstrates the potential of HOF-based cell encapsulation and transplantation as a promising strategy for the treatment of impaired neural networks, particularly in the context of neurodegenerative diseases like Alzheimer's disease.

### 3.5 Proton conductivity

HOFs are excellent candidates for proton conductors due to their intrinsic H-bonding networks. In general, the structural diversity of HOFs allows for the construction of a well-defined H-bonding network in the structure, either in the host framework or from guest molecules, which enables proton motion. A large number of studies have demonstrated the advantages of HOFs as a platform for proton conductors.<sup>110–116</sup> For example, in 2011, Kim *et al.* reported proton conductivity in organic molecular porous materials based on cucurbituril (CB) compounds.<sup>115</sup> Among them, CB[6]·H<sub>2</sub>SO<sub>4</sub> exhibited the highest proton conductivities at 98% RH and 298 K with a value of  $1.3 \times 10^{-3}$  S cm<sup>-1</sup>, representing one of the pioneering studies that demonstrated the application of HOFs in this area. Another important study reported by Ghosh *et al.* described two porous HOFs, HOF-GS-10 and HOF-GS-11, based on arene sulfonates and guanidinium ions. The materials show high proton conduction values of  $0.75 \times 10^{-2}$  S cm<sup>-1</sup> and  $1.8 \times 10^{-2}$  S cm<sup>-1</sup> under humidified conditions.<sup>114</sup> Although the flexible behavior of HOFs in proton conduction is not always visible, the simplicity of processing and regeneration due to their flexibility also benefits this application.

In 2023, our group reported a 2D layered structure by constructing a donor-acceptor  $\pi$ - $\pi$  stacked HOF (HOF-FJU-36) utilizing 1,1'-bis(3-carboxyphenylmethyl)-4,4'-bipyridine (H<sub>2</sub>L<sup>2+</sup>) as the acceptor and 2,7-naphthalene disulfonate (NDS<sup>2-</sup>) as the donor.<sup>112</sup> The presence of three water molecules in the channel, interconnecting the acids by H-bonding, forms a 3D framework. Continuous  $\pi$ - $\pi$  interactions along the *a*-axis direction and smooth H-bonding chains along the *b*-axis direction provide pathways for electron and proton transport. After 405 nm illumination, the photogenerated radicals were able to give HOF-FJU-36 both switchable electron and proton conductivity due to



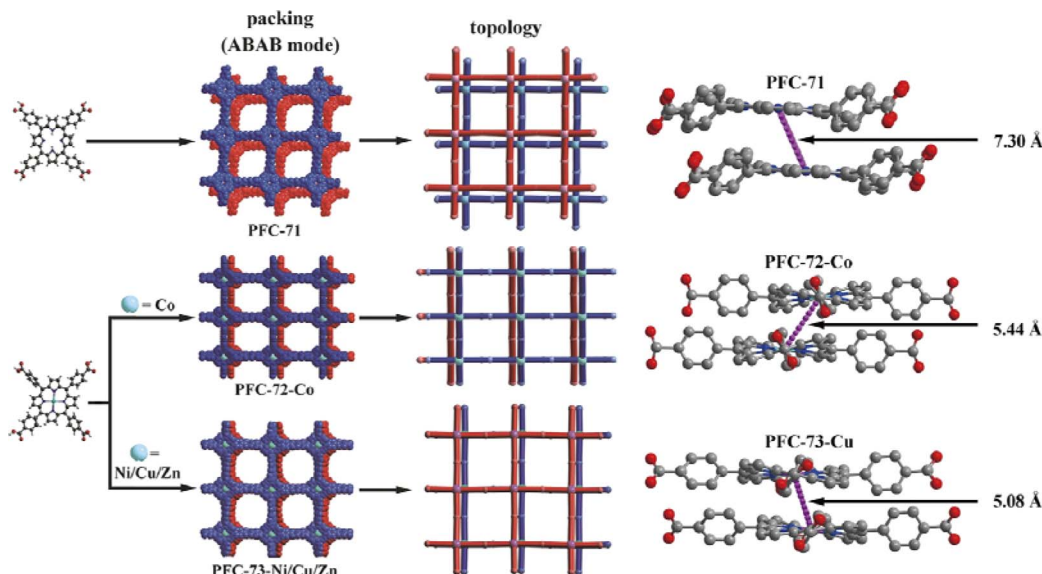


Fig. 19 (left) Schematic representation of the structure and topology of PFC-71, PFC72-Co, and PFC-73-Ni/Cu/Zn; (right) the interlayer porphyrin center-to-center distance of PFC-71, PFC72-Co, and PFC-73-Cu.<sup>61</sup>

coupled electron-proton transfer. This work demonstrated that by rationally designing flexible HOFs, the coupling of proton-electron transfer can be realized, resulting in controllable photoresponsive electronic and proton conductivity.

### 3.6 Other applications

Further research on flexible HOFs remains ongoing, and their applications involve many areas that will not be detailed here, such as catalysis,<sup>61,117–122</sup> chiral separation,<sup>123,124</sup> etc.

In 2022, Liu *et al.* reported the synthesis and characterization of porphyrin-based HOFs (PFC-71, PFC-72, and PFC-73) for photocatalytic CO<sub>2</sub> reduction.<sup>61</sup> [5,10,15,20-tetrakis(4-carboxyphenyl)porphyrin] (TCPP) is applied to synthesize these HOFs with different metallized porphyrin centers. In the case of PFC-71, the porphyrin center is not metallized, whereas, in PFC-72, PFC-73-Ni, PFC-73-Cu, and PFC-73-Zn, the porphyrin center is metallized with different metal ions (Co, Ni, Cu, and Zn, respectively). This metallization of the porphyrin center leads to a larger electronegativity difference on the macrocycle backbone, causing increased polarizability and electron cloud distortion, resulting in the formation of stronger offset π–π interactions between adjacent interlamellar porphyrins. PFC-72 and PFC-73 exhibit higher stability compared to PFC-71. The undulated geometry of the metallized layers, along with the deeper interlayer penetrations and orientation of benzene rings orthogonal to the layer, increases the geometrical barrier for sliding and contributes to the higher stability of PFC-72 and PFC-73 (Fig. 19). The authors investigate the metallization process of the HOFs and its effect on the photocatalytic activity, demonstrating the potential of these HOFs as photocatalysts for CO<sub>2</sub> reduction.

### 3.7 Future directions for flexible HOFs' applications

Over the last decade, research on flexible HOFs has demonstrated great potential for diverse applications. In-depth

research into the structure–function relationship has greatly improved the response of flexible HOFs to a broader range of stimuli, particularly in biomedical applications. In recent years, there has been a lot of interest in the development of HOF membranes, and flexible HOFs have the potential to expand the range of applications in this field even further.<sup>125</sup> In addition, researchers are improving the synthesis and processing technologies of flexible HOFs in order to enable further application in industry. Overall, research in the future should concentrate on utilizing the unique features of flexible HOFs to provide inventive solutions for a variety of practical applications.

## 4. Conclusions and outlook

In this perspective, we have summarized and analyzed the very common and interesting phenomenon of flexibility in HOFs. We believe that flexibility refers to the ability or range of deformability of the overall or local structure, *i.e.*, the ability to undergo structural changes or deformations under certain stimuli without losing (or restoring) its crystallinity or function. This flexibility allows HOFs to be adapted to different environments and applications. We should note that the flexibility of HOFs differs notably from that of MOFs and COFs. First, the flexibility of HOFs mainly comes from the flexibility and reversibility of H-bonding. H-bonding is important for HOFs' flexible behavior, and they can be distorted, broken, and reformed in response to external stimuli, which is a unique property of HOFs. MOFs, on the other hand, are typically flexible due to their metal–organic coordination bonds between metal ions and organic ligands, which can undergo stretching or rotation to some extent, making MOFs flexible to a limited degree. COFs are composed of organic molecules connected by covalent bonds that can be bent or twisted under external stresses, allowing them some deformability. The distinctive features of flexible HOFs endow them with some special



advantages, but they also pose challenges for their design and application.

Currently, the challenges of flexible HOFs mainly focus on: (1) the complexity of structural design; (2) framework stability; (3) controlling H-bond dynamic behaviour. Designing flexible HOFs requires precise control of the structure and arrangement of organic molecules to ensure that the framework can undergo reversible changes. However, flexible HOFs usually have lower structural stability due to the flexible and reversible nature of H-bonding, and thus, the relationship between flexibility and stability needs to be balanced in the design. At the same time, it is essential to explore how to effectively control the kinetic behaviour of H-bonds to achieve the desired structure change and performance.

HOFs are still facing challenges and opportunities in their applications. Although typically HOFs are not as stable as MOFs and HOFs in terms of their structure rigidity and thus porosity, some HOFs can indeed be very stable even under highly acidic/basic conditions and high temperatures, particularly when framework interpenetration and other weak interactions such as  $\pi\cdots\pi$  and C-H $\cdots\pi$  can collaboratively reinforce the HOF framework. The simple recrystallization nature of most HOF materials can allow us to easily and straightforwardly regenerate HOF materials for their reusage, which will save the material costs for some of their applications, particularly in gas storage and separation, and catalysis. Apparently, HOFs are not as designable as MOFs and HOFs, so extensive exploration of different synthetic approaches is still necessary to discover some unique HOF materials for different applications. To make use of the framework flexibility, we can execute more parameters through changing the temperatures and pressures to finely tune and maximize the gas separation and purification, targeting some functional HOF materials for gas separation/purification even without our imagination. Because HOFs purely contain only organic species and can be reversibly dissociated/re-assembled, their compatibility with biological systems is expected to be better than that of MOFs and COFs. HOFs also do not have metal ion species, and this might be another advantage for HOFs for their biomedical applications. Given the fact that HOF structures can be easily stimulated even by some very weak external stimuli such as light and ultrasonic irradiation, HOFs are very promising materials for drug delivery and thus for the treatment of some challenging diseases. As fast development in MOF chemistry and materials science, HOF composite materials will be also developed in the near future for their broad applications. In conclusion, flexible HOFs will provide us with the bright promise to design and construct many HOF materials for a variety of applications. We believe that some flexible HOF materials might be eventually implemented in practical applications in energy and environmental science and biomedical applications in the future.

## Author contributions

J. L. and B. C. performed the literature search, analyzed the published results, and wrote the manuscript.

## Conflicts of interest

There are no conflicts to declare.

## Acknowledgements

Jiantang Li acknowledges the support of the National Natural Science Foundation of China (No. 22301154).

## Notes and references

- 1 M. A. Little and A. I. Cooper, The Chemistry of Porous Organic Molecular Materials, *Adv. Funct. Mater.*, 2020, **30**, 1909842.
- 2 T. D. Bennett, F. X. Coudert, S. L. James and A. I. Cooper, The changing state of porous materials, *Nat. Mater.*, 2021, **20**, 1179–1187.
- 3 R. Freund, S. Canossa, S. M. Cohen, W. Yan, H. Deng, V. Guillerm, M. Eddaoudi, D. G. Madden, D. Fairen-Jimenez, H. Lyu, L. K. Macreadie, Z. Ji, Y. Zhang, B. Wang, F. Haase, C. Woll, O. Zaremba, J. Andreo, S. Wuttke and C. S. Diercks, 25 Years of Reticular Chemistry, *Angew. Chem., Int. Ed.*, 2021, **60**, 23946–23974.
- 4 H. Jiang, D. Alezi and M. Eddaoudi, A reticular chemistry guide for the design of periodic solids, *Nat. Rev. Mater.*, 2021, **6**, 466–487.
- 5 H. L. Nguyen, Reticular design and crystal structure determination of covalent organic frameworks, *Chem. Sci.*, 2021, **12**, 8632–8647.
- 6 J. Kim and W. Choe, Topology-guided roadmap for reticular chemistry of metal-organic polyhedra, *Chem.*, 2022, **8**, 617–631.
- 7 A. G. Slater and A. I. Cooper, Porous materials. Function-led design of new porous materials, *Science*, 2015, **348**, aaa8075.
- 8 U. Díaz and A. Corma, Ordered covalent organic frameworks, COFs and PAFs. From preparation to application, *Coord. Chem. Rev.*, 2016, **311**, 85–124.
- 9 T. Hasell and A. I. Cooper, Porous organic cages: soluble, modular and molecular pores, *Nat. Rev. Mater.*, 2016, **1**, 16053.
- 10 I. Hisaki, C. Xin, K. Takahashi and T. Nakamura, Designing Hydrogen-Bonded Organic Frameworks (HOFs) with Permanent Porosity, *Angew. Chem., Int. Ed.*, 2019, **58**, 11160–11170.
- 11 R. B. Lin, Y. He, P. Li, H. Wang, W. Zhou and B. Chen, Multifunctional porous hydrogen-bonded organic framework materials, *Chem. Soc. Rev.*, 2019, **48**, 1362–1389.
- 12 B. Wang, R. B. Lin, Z. Zhang, S. Xiang and B. Chen, Hydrogen-Bonded Organic Frameworks as a Tunable Platform for Functional Materials, *J. Am. Chem. Soc.*, 2020, **142**, 14399–14416.
- 13 R. B. Lin and B. L. Chen, Hydrogen-bonded organic frameworks: Chemistry and functions, *Chem.*, 2022, **8**, 2114–2135.
- 14 X. Song, Y. Wang, C. Wang, D. Wang, G. Zhuang, K. O. Kirlikovali, P. Li and O. K. Farha, Design Rules of Hydrogen-Bonded Organic Frameworks with High



Chemical and Thermal Stabilities, *J. Am. Chem. Soc.*, 2022, **144**, 10663–10687.

15 Y. Liu, G. Chang, F. Zheng, L. Chen, Q. Yang, Q. Ren and Z. Bao, Hybrid Hydrogen-Bonded Organic Frameworks: Structures and Functional Applications, *Chem.-Eur. J.*, 2023, **29**, e202202655.

16 P. Soleimani Abhari, S. Gholizadeh, F. Rouhani, Y.-L. Li, A. Morsali and T.-F. Liu, Recent progress in gas separation platforms based on hydrogen-bonded organic frameworks (HOFs), *Inorg. Chem. Front.*, 2023, **10**, 6134–6159.

17 M. C. Das, S. C. Pal and B. Chen, Emerging microporous HOF materials to address global energy challenges, *Joule*, 2022, **6**, 22–27.

18 Z. S. Zhang and B. Yan, Smart Multiple Photoresponsive Tongue for Sensing Umami, Sour and Bitter Tastes Based on Tb Functionalized Hydrogen-Bonded Organic Frameworks, *Adv. Funct. Mater.*, 2024, DOI: [10.1002/adfm.202316195](https://doi.org/10.1002/adfm.202316195).

19 L. Zhang, Y. T. Luo, S. J. Xiao, J. Q. Fan, Q. G. Tan, C. Sun, A. M. Song, R. P. Liang and J. D. Qiu, The construction of a stable hydrogen-bonded organic framework for the photocatalytic reduction and removal of uranium, *Chem. Commun.*, 2024, **60**, 3583–3586.

20 Q. Yin, K. Pang, Y. N. Feng, L. Han, A. Morsali, X. Y. Li and T. F. Liu, Hydrogen-bonded organic frameworks in solution enables continuous and high-crystalline membranes, *Nat. Commun.*, 2024, **15**, 634.

21 W. Z. Luo, J. Y. Zhou, Y. J. Nie, F. M. Li, S. Y. Cai, G. Q. Yin, T. Chen and Z. X. Cai, Hydrogen-Bonded Organic Frameworks Enabling Highly Robust Aqueous Phase Ultralong Room-Temperature Phosphorescence, *Adv. Funct. Mater.*, 2024, DOI: [10.1002/adfm.202401728](https://doi.org/10.1002/adfm.202401728).

22 C. F. Guo, Y. Gao, S. Q. Li, Y. X. Wang, X. J. Yang, C. W. Zhi, H. Zhang, Y. F. Zhu, S. Q. Chen, S. L. Chou, S. X. Dou, Y. Xiao and X. P. Luo, Chemical-Stabilized Aldehyde-Tuned Hydrogen-Bonded Organic Frameworks for Long-Cycle and High-Rate Sodium-Ion Organic Batteries, *Adv. Funct. Mater.*, 2024, **34**, 2314851.

23 A. P. Dianin, Condensation of phenol with unsaturated ketones. Condensation of phenol with mesityl oxide, *Zh. Russ. Fiz.-Khim. O-va.*, 1914, **46**, 1310.

24 H. Li, M. Eddaoudi, T. L. Groy and O. M. Yaghi, Establishing Microporosity in Open Metal–Organic Frameworks: Gas Sorption Isotherms for Zn(BDC) (BDC = 1,4-Benzenedicarboxylate), *J. Am. Chem. Soc.*, 1998, **120**, 8571–8572.

25 P. Brunet, M. Simard and J. D. Wuest, Molecular tectonics. Porous hydrogen-bonded networks with unprecedented structural integrity, *J. Am. Chem. Soc.*, 1997, **119**, 2737–2738.

26 M. Gallant, T. Phan Viet Minh and J. D. Wuest, Use of hydrogen bonds to control molecular aggregation. Association of dipyridones joined by flexible spacers, *J. Org. Chem.*, 1991, **56**, 2284–2286.

27 Y. He, S. Xiang and B. Chen, A microporous hydrogen-bonded organic framework for highly selective  $C_2H_2/C_2H_4$  separation at ambient temperature, *J. Am. Chem. Soc.*, 2011, **133**, 14570–14573.

28 W. Yang, A. Greenaway, X. Lin, R. Matsuda, A. J. Blake, C. Wilson, W. Lewis, P. Hubberstey, S. Kitagawa, N. R. Champness and M. Schroder, Exceptional thermal stability in a supramolecular organic framework: porosity and gas storage, *J. Am. Chem. Soc.*, 2010, **132**, 14457–14469.

29 A. E. Amooghin, H. Sanaeepur, M. Ghomi, R. Luque, H. Garcia and B. Chen, Flexible-robust MOFs/HOFs for challenging gas separations, *Coord. Chem. Rev.*, 2024, **505**, 215660.

30 S. Krause, N. Hosono and S. Kitagawa, Chemistry of Soft Porous Crystals: Structural Dynamics and Gas Adsorption Properties, *Angew. Chem., Int. Ed.*, 2020, **59**, 15325–15341.

31 J. H. Lee, S. Jeoung, Y. G. Chung and H. R. Moon, Elucidation of flexible metal-organic frameworks: Research progresses and recent developments, *Coord. Chem. Rev.*, 2019, **389**, 161–188.

32 S. K. Elsaidi, M. H. Mohamed, D. Banerjee and P. K. Thallapally, Flexibility in Metal-Organic Frameworks: A fundamental understanding, *Coord. Chem. Rev.*, 2018, **358**, 125–152.

33 A. Schneemann, V. Bon, I. Schwedler, I. Senkovska, S. Kaskel and R. A. Fischer, Flexible metal-organic frameworks, *Chem. Soc. Rev.*, 2014, **43**, 6062–6096.

34 Z.-J. Lin, J. Lu, M. Hong and R. Cao, Metal-organic frameworks based on flexible ligands (FL-MOFs): structures and applications, *Chem. Soc. Rev.*, 2014, **43**, 5867–5895.

35 C. A. Zentner, H. W. H. Lai, J. T. Greenfield, R. A. Wiscons, M. Zeller, C. F. Campana, O. Talu, S. A. FitzGerald and J. L. C. Rowsell, High surface area and Z' in a thermally stable 8-fold polycatenated hydrogen-bonded framework, *Chem. Commun.*, 2015, **51**, 11642–11645.

36 T. Liu, B. Wang, R. He, H. Arman, K. S. Schanze, S. C. Xiang, D. Li and B. L. Chen, A novel hydrogen-bonded organic framework for the sensing of two representative organic arsenics, *Can. J. Chem.*, 2020, **98**, 352–357.

37 Y. L. Li, E. V. Alexandrov, Q. Yin, L. Li, Z. B. Fang, W. B. Yuan, D. M. Proserpio and T. F. Liu, Record Complexity in the Polycatenation of Three Porous Hydrogen-Bonded Organic Frameworks with Stepwise Adsorption Behaviors, *J. Am. Chem. Soc.*, 2020, **142**, 7218–7224.

38 J. Gao, Y. Cai, X. Qian, P. Liu, H. Wu, W. Zhou, D. X. Liu, L. Li, R. B. Lin and B. Chen, A Microporous Hydrogen-Bonded Organic Framework for the Efficient Capture and Purification of Propylene, *Angew. Chem., Int. Ed.*, 2021, **60**, 20400–20406.

39 J. T. A. Jones, T. Hasell, X. Wu, J. Bacsa, K. E. Jelfs, M. Schmidtmann, S. Y. Chong, D. J. Adams, A. Trewin, F. Schiffman, F. Cora, B. Slater, A. Steiner, G. M. Day and A. I. Cooper, Modular and predictable assembly of porous organic molecular crystals, *Nature*, 2011, **474**, 367–371.

40 P. Li, Y. He, H. D. Arman, R. Krishna, H. Wang, L. Weng and B. Chen, A microporous six-fold interpenetrated hydrogen-



bonded organic framework for highly selective separation of  $C_2H_4/C_2H_6$ , *Chem. Commun.*, 2014, **50**, 13081–13084.

41 X. Zhang, J. X. Wang, L. Li, J. Pei, R. Krishna, H. Wu, W. Zhou, G. Qian, B. Chen and B. Li, A Rod-Pack Hydrogen-Bonded Organic Framework with Suitable Pore Confinement for Benchmark Ethane/Ethylene Separation, *Angew. Chem., Int. Ed.*, 2021, **60**, 10304–10310.

42 L. Gong, Y. Ye, Y. Liu, Y. Li, Z. Bao, S. Xiang, Z. Zhang and B. Chen, A Microporous Hydrogen-Bonded Organic Framework for Efficient  $Xe/Kr$  Separation, *ACS Appl. Mater. Interfaces*, 2022, **14**, 19623–19628.

43 Z. Yuan, X. Jiang, L. Chen, J. Chen, L. Li, Y. Yang, Y. Li, F. Xiang, S. Xiang, B. Chen and Z. Zhang, Sticked-Layer Strategy to a Flexible-Robust Hydrogen-Bonded Organic Framework for Efficient  $C_2H_2/CO_2$  Separation, *CCS Chem.*, 2024, **6**, 663–671.

44 D. D. Zhou, Y. T. Xu, R. B. Lin, Z. W. Mo, W. X. Zhang and J. P. Zhang, High-symmetry hydrogen-bonded organic frameworks: air separation and crystal-to-crystal structural transformation, *Chem. Commun.*, 2016, **52**, 4991–4994.

45 H. Wang, B. Li, H. Wu, T. L. Hu, Z. Yao, W. Zhou, S. Xiang and B. Chen, A Flexible Microporous Hydrogen-Bonded Organic Framework for Gas Sorption and Separation, *J. Am. Chem. Soc.*, 2015, **137**, 9963–9970.

46 W. Yang, B. Li, H. L. Wang, O. Alduhaish, K. Alfooty, M. A. Zayed, P. Li, H. D. Arman and B. L. Chen, A Microporous Porphyrin-Based Hydrogen-Bonded Organic Framework for Gas Separation, *Cryst. Growth Des.*, 2015, **15**, 2000–2004.

47 Q. Huang, W. Li, Z. Mao, L. Qu, Y. Li, H. Zhang, T. Yu, Z. Yang, J. Zhao, Y. Zhang, M. P. Aldred and Z. Chi, An exceptionally flexible hydrogen-bonded organic framework with large-scale void regulation and adaptive guest accommodation abilities, *Nat. Commun.*, 2019, **10**, 3074.

48 Q. Y. Huang, W. L. Li, Z. Mao, H. Zhang, Y. Li, D. Y. Ma, H. Y. Wu, J. Zhao, Z. Y. Yang, Y. Zhang, G. Li, M. P. Aldred and Z. G. Chi, Dynamic molecular weaving in a two-dimensional hydrogen-bonded organic framework, *Chem.*, 2021, **7**, 1321–1332.

49 W. Yang, F. Yang, T. L. Hu, S. C. King, H. L. Wang, H. Wu, W. Zhou, J. R. Li, H. D. Arman and B. L. Chen, Microporous Diaminotriazine-Decorated Porphyrin-Based Hydrogen-Bonded Organic Framework: Permanent Porosity and Proton Conduction, *Cryst. Growth Des.*, 2016, **16**, 5831–5835.

50 P. Li, P. Li, M. R. Ryder, Z. Liu, C. L. Stern, O. K. Farha and J. F. Stoddart, Interpenetration Isomerism in Triptycene-Based Hydrogen-Bonded Organic Frameworks, *Angew. Chem., Int. Ed.*, 2019, **58**, 1664–1669.

51 W. Yang, W. Zhou and B. L. Chen, A Flexible Microporous Hydrogen-Bonded Organic Framework, *Cryst. Growth Des.*, 2019, **19**, 5184–5188.

52 Y. Yang, L. Li, R. B. Lin, Y. Ye, Z. Yao, L. Yang, F. Xiang, S. Chen, Z. Zhang, S. Xiang and B. Chen, Ethylene/ethane separation in a stable hydrogen-bonded organic framework through a gating mechanism, *Nat. Chem.*, 2021, **13**, 933–939.

53 Y. Chen, Y. Yang, Y. Wang, Q. Xiong, J. Yang, S. Xiang, L. Li, J. Li, Z. Zhang and B. Chen, Ultramicroporous Hydrogen-Bonded Organic Framework Material with a Thermoregulatory Gating Effect for Record Propylene Separation, *J. Am. Chem. Soc.*, 2022, **144**, 17033–17040.

54 Y. Yang, H. Zhang, Z. Yuan, J. Q. Wang, F. Xiang, L. Chen, F. Wei, S. Xiang, B. Chen and Z. Zhang, An Ultramicroporous Hydrogen-Bonded Organic Framework Exhibiting High  $C_2H_2/CO_2$  Separation, *Angew. Chem., Int. Ed.*, 2022, **61**, e202207579.

55 C. Jiang, J.-X. Wang, D. Liu, E. Wu, X.-W. Gu, X. Zhang, B. Li, B. Chen and G. Qian, Supramolecular Entanglement in a Hydrogen-Bonded Organic Framework Enables Flexible-Robust Porosity for Highly Efficient Purification of Natural Gas, *Angew. Chem., Int. Ed.*, 2024, DOI: [10.1002/anie.202404734](https://doi.org/10.1002/anie.202404734).

56 I. Hisaki, S. Nakagawa, N. Ikenaka, Y. Imamura, M. Katouda, M. Tashiro, H. Tsuchida, T. Ogoshi, H. Sato, N. Tohnai and M. Miyata, A Series of Layered Assemblies of Hydrogen-Bonded, Hexagonal Networks of  $C_3$ -Symmetric pi-Conjugated Molecules: A Potential Motif of Porous Organic Materials, *J. Am. Chem. Soc.*, 2016, **138**, 6617–6628.

57 L. Ma, Y. Xie, R. S. H. Khoo, H. Arman, B. Wang, W. Zhou, J. Zhang, R. B. Lin and B. Chen, An Adaptive Hydrogen-Bonded Organic Framework for the Exclusive Recognition of p-Xylene, *Chem.-Eur. J.*, 2022, **28**, e202104269.

58 Y. Li, X. Wang, H. Zhang, L. He, J. Huang, W. Wei, Z. Yuan, Z. Xiong, H. Chen, S. Xiang, B. Chen and Z. Zhang, A Microporous Hydrogen Bonded Organic Framework for Highly Selective Separation of Carbon Dioxide over Acetylene, *Angew. Chem., Int. Ed.*, 2023, **62**, e202311419.

59 X. Li, X. Xu, D. Yuan and X. Weng, Hexagonal prismatic dodecameric water cluster: a building unit of the five-fold interpenetrating six-connected supramolecular network, *Chem. Commun.*, 2012, **48**, 9014–9016.

60 B. Yu, S. Geng, H. Wang, W. Zhou, Z. Zhang, B. Chen and J. Jiang, A Solid Transformation into Carboxyl Dimers Based on a Robust Hydrogen-Bonded Organic Framework for Propyne/Propylene Separation, *Angew. Chem., Int. Ed.*, 2021, **60**, 25942–25948.

61 Q. Yin, E. V. Alexandrov, D. H. Si, Q. Q. Huang, Z. B. Fang, Y. Zhang, A. A. Zhang, W. K. Qin, Y. L. Li, T. F. Liu and D. M. Proserpio, Metallization-Prompted Robust Porphyrin-Based Hydrogen-Bonded Organic Frameworks for Photocatalytic  $CO_2$  Reduction, *Angew. Chem., Int. Ed.*, 2022, **61**, e202115854.

62 D. Wang and Y. Zhao, Rigid-Flexible Hybrid Porous Molecular Crystals with Guest-Induced Reversible Crystallinity, *Angew. Chem., Int. Ed.*, 2023, **62**, e202217903.

63 J. Q. Zhao, L. L. Mao, G. H. Zhang, S. Z. Zhan, H. Y. Xiao, S. G. Zhang, C. H. Tung, L. Z. Wu and H. Cong, A polycatenated hydrogen-bonded organic framework based on embraced macrocyclic building blocks for fluorescence





detection of nitrobenzene in water, *J. Mater. Chem. A*, 2023, **11**, 4672–4678.

64 X. Song, Y. Wang, C. Wang, X. Gao, Y. Zhou, B. Chen and P. Li, Self-Healing Hydrogen-Bonded Organic Frameworks for Low-Concentration Ammonia Capture, *J. Am. Chem. Soc.*, 2024, **146**, 627–634.

65 X. Y. Gao, Y. L. Li, T. F. Liu, X. S. Huang and R. Cao, Single-crystal-to-single-crystal transformation of tetrathiafulvalene-based hydrogen-bonded organic frameworks, *CrystEngComm*, 2021, **23**, 4743–4747.

66 L. Chen, Z. Yuan, H. Zhang, Y. Ye, Y. Yang, F. Xiang, K. Cai, S. Xiang, B. Chen and Z. Zhang, A Flexible Hydrogen-Bonded Organic Framework Constructed from a Tetrabenzaldehyde with a Carbazole N-H Binding Site for the Highly Selective Recognition and Separation of Acetone, *Angew. Chem., Int. Ed.*, 2022, **61**, e202213959.

67 Y. Zhou, C. Chen, R. Krishna, Z. Ji, D. Yuan and M. Wu, Tuning Pore Polarization to Boost Ethane/Ethylene Separation Performance in Hydrogen-Bonded Organic Frameworks, *Angew. Chem., Int. Ed.*, 2023, **62**, e202305041.

68 S. Wang, J. Liu, S. Feng, J. Wu, Z. Yuan, B. Chen, Q. Ling and Z. Lin, Anionic Hydrogen-Bonded Frameworks Showing Tautomerism and Colorful Luminescence for the Ultrasensitive Detection of Acetone, *Angew. Chem., Int. Ed.*, 2024, **63**, e202400742.

69 B. Yu, S. Geng, H. Wang, W. Zhou, Z. Zhang, B. Chen and J. Jiang, A Solid Transformation into Carboxyl Dimers Based on a Robust Hydrogen-Bonded Organic Framework for Propyne/Propylene Separation, *Angew. Chem., Int. Ed.*, 2021, **60**, 25942–25948.

70 J. Samanta, R. W. Dorn, W. L. Zhang, X. F. Jiang, M. S. Zhang, R. J. Staples, A. J. Rossini and C. F. Ke, An ultra-dynamic anion-cluster-based organic framework, *Chem.*, 2022, **8**, 253–267.

71 P. Cui, E. Svensson Grape, P. R. Spackman, Y. Wu, R. Clowes, G. M. Day, A. K. Inge, M. A. Little and A. I. Cooper, An Expandable Hydrogen-Bonded Organic Framework Characterized by Three-Dimensional Electron Diffraction, *J. Am. Chem. Soc.*, 2020, **142**, 12743–12750.

72 Q. Y. Huang, X. X. Chen, W. L. Li, Z. Y. Yang, Y. Zhang, J. Zhao and Z. G. Chi, Local dynamics in a hydrogen-bonded organic framework for adaptive guest accommodation with programmable luminescence, *Chem.*, 2023, **9**, 1241–1254.

73 Q. Zhu, L. Wei, C. Zhao, H. Qu, B. Liu, T. Fellowes, S. Yang, A. Longcake, M. J. Hall, M. R. Probert, Y. Zhao, A. I. Cooper and M. A. Little, Soft Hydrogen-Bonded Organic Frameworks Constructed Using a Flexible Organic Cage Hinge, *J. Am. Chem. Soc.*, 2023, **145**, 23352–23360.

74 S. Bourrelly, P. L. Llewellyn, C. Serre, F. Millange, T. Loiseau and G. Ferey, Different adsorption behaviors of methane and carbon dioxide in the isotropic nanoporous metal terephthalates MIL-53 and MIL-47, *J. Am. Chem. Soc.*, 2005, **127**, 13519–13521.

75 T. Loiseau, C. Serre, C. Huguenard, G. Fink, F. Taulelle, M. Henry, T. Bataille and G. Ferey, A rationale for the large breathing of the porous aluminum terephthalate (MIL-53) upon hydration, *Chem.-Eur. J.*, 2004, **10**, 1373–1382.

76 C. Serre, F. Millange, C. Thouvenot, M. Nogues, G. Marsolier, D. Louer and G. Ferey, Very Large Breathing Effect in the First Nanoporous Chromium(III)-Based Solids: MIL-53 or  $\text{Cr}^{\text{III}}(\text{OH}) \cdot \{\text{O}_2\text{C}-\text{C}_6\text{H}_4-\text{CO}_2\} \cdot \{\text{HO}_2\text{C}-\text{C}_6\text{H}_4-\text{CO}_2\text{H}\}_x \cdot \text{H}_2\text{O}_y$ , *J. Am. Chem. Soc.*, 2002, **124**, 13519–13526.

77 M. Gupta and J. J. Vittal, Control of interpenetration and structural transformations in the interpenetrated MOFs, *Coord. Chem. Rev.*, 2021, **435**, 213789.

78 Y.-N. Gong, D.-C. Zhong and T.-B. Lu, Interpenetrating metal-organic frameworks, *CrystEngComm*, 2016, **18**, 2596–2606.

79 Z. Yuan, L. J. Chen, X. Zhou, L. Li, Y. B. Li, Y. S. Yang, Z. Q. Zhou, Y. T. Chen, S. C. Xiang, B. L. Chen and Z. J. Zhang, Hydrogen-bonded organic framework with tailored pores prepared by enlarging the core size for high-performance Xe/Kr separation, *J. Mater. Chem. A*, 2023, **11**, 21857–21863.

80 X. Yu Gao, Y. Wang, E. Wu, C. Wang, B. Li, Y. Zhou, B. Chen and P. Li, Multivariate Hydrogen-Bonded Organic Frameworks with Tunable Permanent Porosities for Capture of a Mustard Gas Simulant, *Angew. Chem., Int. Ed.*, 2023, **62**, e202312393.

81 J. Huang, Y. Li, H. Zhang, Z. Yuan, S. Xiang, B. Chen and Z. Zhang, A Microporous Hydrogen-Bonded Organic Framework Based on Hydrogen-Bonding Tetramers for Efficient Xe/Kr Separation, *Angew. Chem., Int. Ed.*, 2023, **62**, e202315987.

82 Y. L. Cai, H. W. Chen, P. X. Liu, J. Z. Chen, H. Xu, T. Alshahrani, L. B. Li, B. L. Chen and J. K. Gao, Robust microporous hydrogen-bonded organic framework for highly selective purification of methane from natural gas, *Microporous Mesoporous Mater.*, 2023, **352**, 112495.

83 X. Zhang, L. Li, J. X. Wang, H. M. Wen, R. Krishna, H. Wu, W. Zhou, Z. N. Chen, B. Li, G. Qian and B. Chen, Selective Ethane/Ethylene Separation in a Robust Microporous Hydrogen-Bonded Organic Framework, *J. Am. Chem. Soc.*, 2020, **142**, 633–640.

84 B. Wang, X. L. Lv, J. Lv, L. Ma, R. B. Lin, H. Cui, J. Zhang, Z. Zhang, S. Xiang and B. Chen, A novel mesoporous hydrogen-bonded organic framework with high porosity and stability, *Chem. Commun.*, 2019, **56**, 66–69.

85 W. Yang, J. W. Wang, H. L. Wang, Z. B. Bao, J. C. G. Zhao and B. L. Chen, Highly Interpenetrated Robust Microporous Hydrogen-Bonded Organic Framework for Gas Separation, *Cryst. Growth Des.*, 2017, **17**, 6132–6137.

86 H. L. Wang, H. Wu, J. L. Kan, G. G. Chang, Z. Z. Yao, B. Li, W. Zhou, S. C. Xiang, J. C. G. Zhao and B. L. Chen, A microporous hydrogen-bonded organic framework with amine sites for selective recognition of small molecules, *J. Mater. Chem. A*, 2017, **5**, 8292–8296.

87 H. Wang, Z. Bao, H. Wu, R. B. Lin, W. Zhou, T. L. Hu, B. Li, J. C. Zhao and B. Chen, Two solvent-induced porous hydrogen-bonded organic frameworks: solvent effects on

structures and functionalities, *Chem. Commun.*, 2017, **53**, 11150–11153.

88 B. L. Chen, An ultrastable and easily regenerated HOF for the selective storage and separation of light hydrocarbons, *Sci. China: Chem.*, 2017, **60**, 683–684.

89 P. Li, Y. He, Y. Zhao, L. Weng, H. Wang, R. Krishna, H. Wu, W. Zhou, M. O'Keeffe, Y. Han and B. Chen, A rod-packing microporous hydrogen-bonded organic framework for highly selective separation of  $C_2H_2/CO_2$  at room temperature, *Angew. Chem., Int. Ed.*, 2015, **54**, 574–577.

90 Z. Chen, P. Li, R. Anderson, X. Wang, X. Zhang, L. Robison, L. R. Redfern, S. Moribe, T. Islamoglu, D. A. Gomez-Gualdrón, T. Yildirim, J. F. Stoddart and O. K. Farha, Balancing volumetric and gravimetric uptake in highly porous materials for clean energy, *Science*, 2020, **368**, 297–303.

91 R. Natarajan, L. Bridgland, A. Sirikulkajorn, J. H. Lee, M. F. Haddow, G. Magro, B. Ali, S. Narayanan, P. Strickland, J. P. Charmant, A. G. Orpen, N. B. McKeown, C. G. Bezzu and A. P. Davis, Tunable porous organic crystals: structural scope and adsorption properties of nanoporous steroidal ureas, *J. Am. Chem. Soc.*, 2013, **135**, 16912–16925.

92 M. Simard, D. Su and J. D. Wuest, Use of hydrogen bonds to control molecular aggregation. Self-assembly of three-dimensional networks with large chambers, *J. Am. Chem. Soc.*, 2002, **113**, 4696–4698.

93 M. Liang, S. Hu, N. Zhou, Z. Liu, Q. Chen, X. Chen, X. Liu, C. P. Li, J. Hao and P. Xue, Flexible Luminescent Hydrogen-bonded Organic Framework for the Separation of Benzene and Cyclohexane, *Small*, 2023, **19**, e2304340.

94 C. Wang, X. Song, Y. Wang, R. Xu, X. Gao, C. Shang, P. Lei, Q. Zeng, Y. Zhou, B. Chen and P. Li, A Solution-Processable Porphyrin-Based Hydrogen-Bonded Organic Framework for Photoelectrochemical Sensing of Carbon Dioxide, *Angew. Chem., Int. Ed.*, 2023, **62**, e202311482.

95 L. Chen, Z. Yuan, F. Feng, X. Zhou, Z. Xiong, W. Wei, H. Zhang, B. Chen, S. Xiang and Z. Zhang, A hydrogen-bonded organic framework containing fluorescent carbazole and responsive pyridyl units for sensing organic acids, *Chin. Chem. Lett.*, 2023, DOI: [10.1016/j.cclet.2023.109344](https://doi.org/10.1016/j.cclet.2023.109344).

96 F. Q. Chen, H. Xu, Y. L. Cai, P. L. Shen, W. H. Zhang, T. Alshahrani, G. X. Bai, S. Q. Xu, B. L. Chen and J. K. Gao, Ratiometric fluorescent sensor for sensitive detection of 3-methoxytyramine based on hydrogen-bonded organic framework, *J. Solid State Chem.*, 2023, **323**, 124036.

97 F. Q. Chen, Y. L. Cai, P. L. Shen, G. X. Bai, T. Alshahrani, J. K. Gao, B. L. Chen, S. Q. Xu and H. Xu, A porous hydrogen-bonded organic framework for sensitive and highly selective fluorescence sensing of carcinoid biomarkers, *Microporous Mesoporous Mater.*, 2023, **361**, 112759.

98 Z. J. Lin, J. Y. Qin, X. P. Zhan, K. Wu, G. J. Cao and B. Chen, Robust Mesoporous Functional Hydrogen-Bonded Organic Framework for Hypochlorite Detection, *ACS Appl. Mater. Interfaces*, 2022, **14**, 21098–21105.

99 B. Wang, R. He, L. H. Xie, Z. J. Lin, X. Zhang, J. Wang, H. Huang, Z. Zhang, K. S. Schanze, J. Zhang, S. Xiang and B. Chen, Microporous Hydrogen-Bonded Organic Framework for Highly Efficient Turn-Up Fluorescent Sensing of Aniline, *J. Am. Chem. Soc.*, 2020, **142**, 12478–12485.

100 X. Ding, J. Chen and G. Ye, Supramolecular polynuclear clusters sustained cubic hydrogen bonded frameworks with octahedral cages for reversible photochromism, *Nat. Commun.*, 2024, **15**, 2782.

101 I. Hisaki, Y. Suzuki, E. Gomez, Q. Ji, N. Tohnai, T. Nakamura and A. Douhal, Acid Responsive Hydrogen-Bonded Organic Frameworks, *J. Am. Chem. Soc.*, 2019, **141**, 2111–2121.

102 Y. Han, T. Zhang, X. Chen, Q. Chen, J. Hao, W. Song, Y. Zeng and P. Xue, Guest-Regulated Luminescence and Force-Stimuli Response of a Hydrogen-Bonded Organic Framework, *ACS Appl. Mater. Interfaces*, 2021, **13**, 32270–32277.

103 C. Ye, T. Zhou, Y. Deng, S. Wu, T. Zeng, J. Yang, Y. S. Shi, Y. Yin and G. Li, Enhanced performance of enzymes confined in biocatalytic hydrogen-bonded organic frameworks for sensing of glutamate in the central nervous system, *Biosens. Bioelectron.*, 2024, **247**, 115963.

104 D. Yu, H. Zhang, J. Ren and X. Qu, Hydrogen-bonded organic frameworks: new horizons in biomedical applications, *Chem. Soc. Rev.*, 2023, **52**, 7504–7523.

105 L. Li, T. Ma and M. Wang, Protein-Integrated Hydrogen-Bonded Organic Frameworks: Chemistry and Biomedical Applications, *Angew. Chem., Int. Ed.*, 2024, e202400926, DOI: [10.1002/anie.202400926](https://doi.org/10.1002/anie.202400926).

106 W. Liang, F. Carraro, M. B. Solomon, S. G. Bell, H. Amenitsch, C. J. Summy, N. G. White, P. Falcaro and C. J. Doonan, Enzyme Encapsulation in a Porous Hydrogen-Bonded Organic Framework, *J. Am. Chem. Soc.*, 2019, **141**, 14298–14305.

107 Q. Yin, P. Zhao, R. J. Sa, G. C. Chen, J. Lu, T. F. Liu and R. Cao, An Ultra-Robust and Crystalline Redeemable Hydrogen-Bonded Organic Framework for Synergistic Chemo-Photodynamic Therapy, *Angew. Chem., Int. Ed.*, 2018, **57**, 7691–7696.

108 G. Chen, L. Tong, S. Huang, S. Huang, F. Zhu and G. Ouyang, Hydrogen-bonded organic framework biomimetic entrapment allowing non-native biocatalytic activity in enzyme, *Nat. Commun.*, 2022, **13**, 4816.

109 D. Yu, H. Zhang, Z. Liu, C. Liu, X. Du, J. Ren and X. Qu, Hydrogen-Bonded Organic Framework (HOF)-Based Single-Neural Stem Cell Encapsulation and Transplantation to Remodel Impaired Neural Networks, *Angew. Chem., Int. Ed.*, 2022, **61**, e202201485.

110 J. J. Yang, J. B. Yin, Q. L. Guo, C. S. Xie, Q. Q. Yang, Z. H. Kong, Z. X. Kang, R. M. Wang and D. F. Sun, Guest-induced proton conductivity of two-dimensional layered hydrogen-bonded organic frameworks, *Inorg. Chem. Front.*, 2023, **10**, 6262–6268.



111 X. L. Wang, L. F. Liang, S. Dou and X. M. Zhang, Two-in-one tecton strategy to construct single crystalline hydrogen-bonded organic framework with high proton conductivity above 100 °C, *Sci. China: Chem.*, 2023, **66**, 2563–2568.

112 S. Chen, Y. Ju, H. Zhang, Y. Zou, S. Lin, Y. Li, S. Wang, E. Ma, W. Deng, S. Xiang, B. Chen and Z. Zhang, Photo Responsive Electron and Proton Conductivity within a Hydrogen-Bonded Organic Framework, *Angew. Chem., Int. Ed.*, 2023, **62**, e202308418.

113 Y. Wang, M. Zhang, Q. Yang, J. Yin, D. Liu, Y. Shang, Z. Kang, R. Wang, D. Sun and J. Jiang, Single-crystal-to-single-crystal transformation and proton conductivity of three hydrogen-bonded organic frameworks, *Chem. Commun.*, 2020, **56**, 15529–15532.

114 A. Karmakar, R. Illathvalappil, B. Anothumakkool, A. Sen, P. Samanta, A. V. Desai, S. Kurungot and S. K. Ghosh, Hydrogen-Bonded Organic Frameworks (HOFs): A New Class of Porous Crystalline Proton-Conducting Materials, *Angew. Chem., Int. Ed.*, 2016, **55**, 10667–10671.

115 M. Yoon, K. Suh, H. Kim, Y. Kim, N. Selvapalam and K. Kim, High and highly anisotropic proton conductivity in organic molecular porous materials, *Angew. Chem., Int. Ed.*, 2011, **50**, 7870–7873.

116 S. C. Pal, D. Mukherjee, R. Sahoo, S. Mondal and M. C. Das, Proton-Conducting Hydrogen-Bonded Organic Frameworks, *ACS Energy Lett.*, 2021, **6**, 4431–4453.

117 J. J. Li, Q. Yin, S. Y. Gao, Y. A. Feng, S. H. Ye, H. F. Li and R. Cao, In Situ Self-Assembly of Hydrogen-Bonded Organic Frameworks for Organic Photoredox Catalysis, *ACS Sustainable Chem. Eng.*, 2023, **11**, 4389–4397.

118 S. Y. Huang, Y. Chang, Z. W. Li, J. Q. Cao, Y. R. Song, J. F. Gao, L. C. Sun and J. A. Hou, Single-Atom Metal Sites Anchored Hydrogen-Bonded Organic Frameworks for Superior “Two-In-One” Photocatalytic Reaction, *Adv. Funct. Mater.*, 2023, **33**, 2211631.

119 L. Feng, Y. Yuan, B. Yan, T. Feng, Y. Jian, J. Zhang, W. Sun, K. Lin, G. Luo and N. Wang, Halogen hydrogen-bonded organic framework (XHOF) constructed by singlet open-shell diradical for efficient photoreduction of U(VI), *Nat. Commun.*, 2022, **13**, 1389.

120 X. Cheng, J. Zhang, Y. Sha, M. Xu, R. Duan, Z. Su, J. Li, Y. Wang, J. Hu, B. Guan and B. Han, Periodically nanoporous hydrogen-bonded organic frameworks for high performance photocatalysis, *Nanoscale*, 2022, **14**, 9762–9770.

121 B. Yu, L. Li, S. Liu, H. Wang, H. Liu, C. Lin, C. Liu, H. Wu, W. Zhou, X. Li, T. Wang, B. Chen and J. Jiang, Robust Biological Hydrogen-Bonded Organic Framework with Post-Functionalized Rhenium(I) Sites for Efficient Heterogeneous Visible-Light-Driven CO<sub>2</sub> Reduction, *Angew. Chem., Int. Ed.*, 2021, **60**, 8983–8989.

122 B. Han, H. Wang, C. Wang, H. Wu, W. Zhou, B. Chen and J. Jiang, Postsynthetic Metalation of a Robust Hydrogen-Bonded Organic Framework for Heterogeneous Catalysis, *J. Am. Chem. Soc.*, 2019, **141**, 8737–8740.

123 W. Wang, Y. Zhang, B. Tang, H. Hou, S. Tang and A. Luo, Chiral hydrogen-bonded organic frameworks used as a chiral stationary phase for chiral separation in gas chromatography, *J. Chromatogr. A*, 2022, **1675**, 463150.

124 P. Li, Y. He, J. Guang, L. Weng, J. C. Zhao, S. Xiang and B. Chen, A homochiral microporous hydrogen-bonded organic framework for highly enantioselective separation of secondary alcohols, *J. Am. Chem. Soc.*, 2014, **136**, 547–549.

125 C. Chen, L. Shen, H. Lin, D. Zhao, B. Li and B. Chen, Hydrogen-bonded organic frameworks for membrane separation, *Chem. Soc. Rev.*, 2024, **53**, 2738–2760.

